

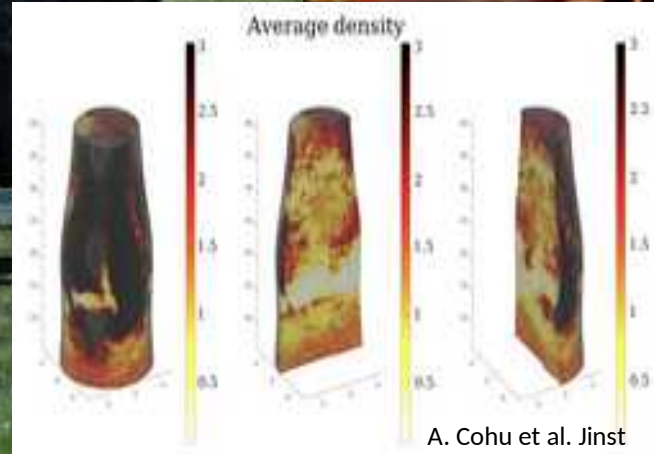
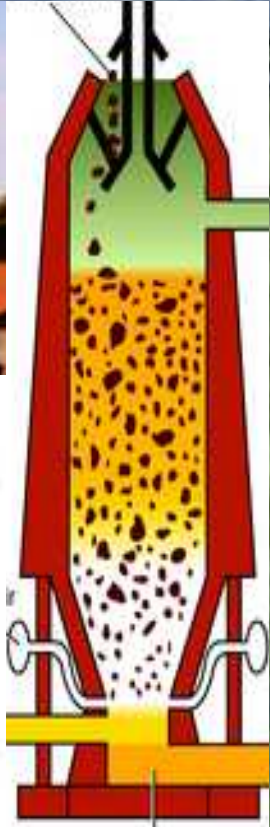
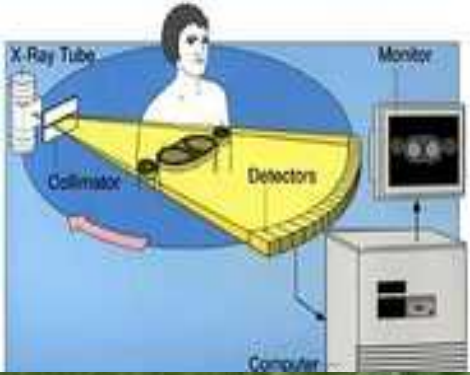
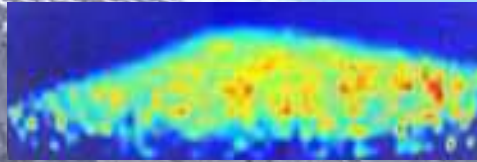
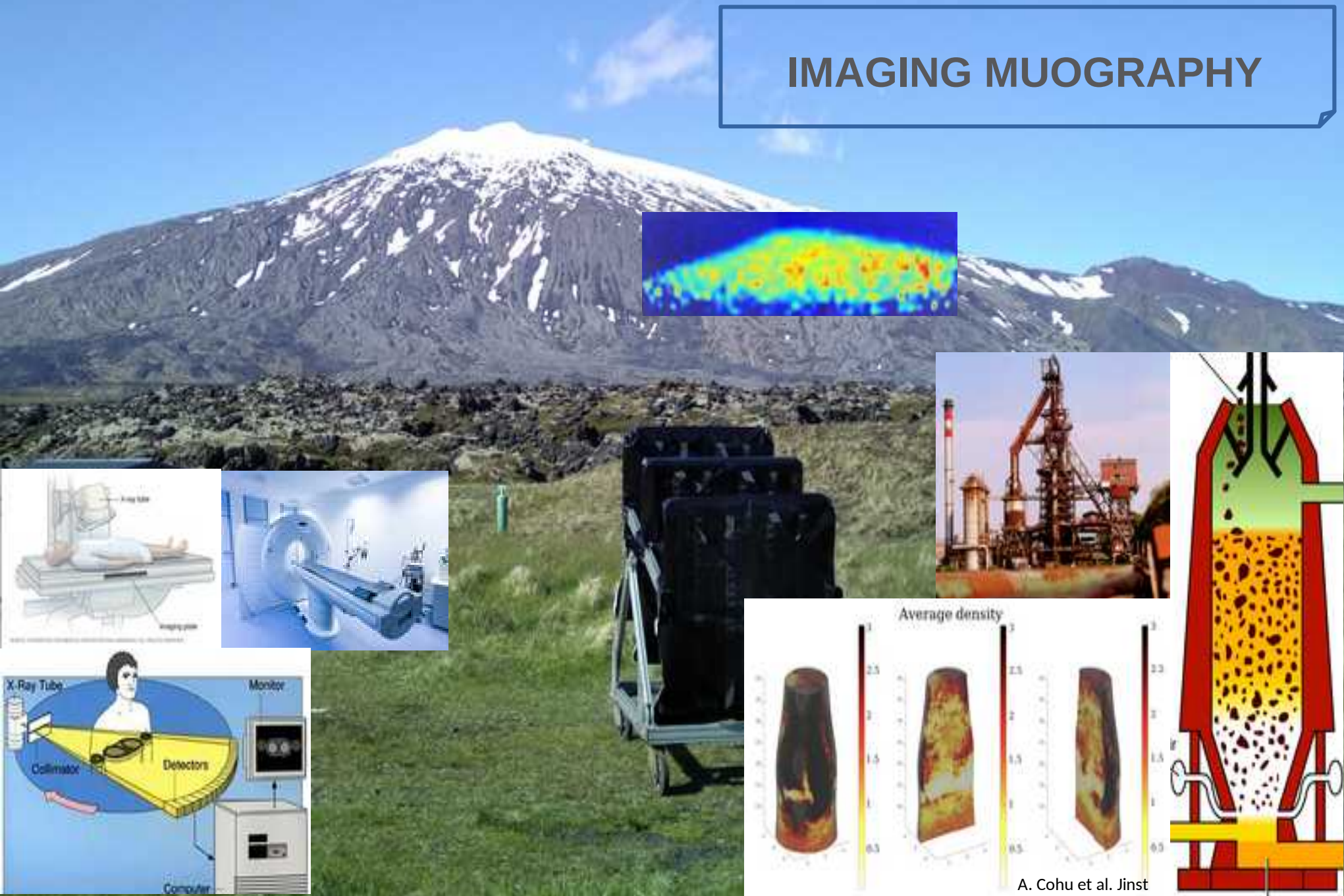


J. Marteau^{1,2}

T.Avgitas¹, D.Caiulo², B.Carlus¹, A.Chevalier², A.Cohu², J.-C.Ianigro^{1,2}, C.Pichol-Thievend²

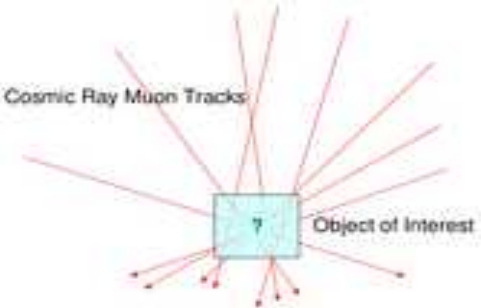
1 – INSTITUT DE PHYSIQUE DES 2 INFINIS DE LYON (IP2I), UNIVERSITÉ LYON-1, CNRS-IN2P3 (UMR5822)
2 – MUODIM, 31 RUE SAINT-MAXIMIN, 69003 LYON

IMAGING MUOGRAPHY

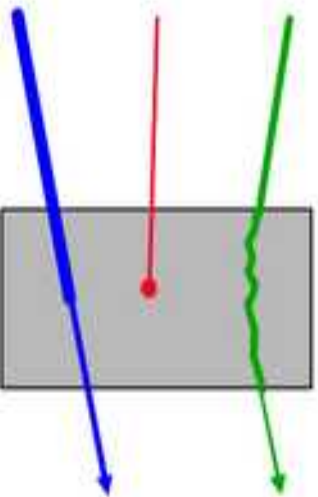


A. Cohu et al. Jinst

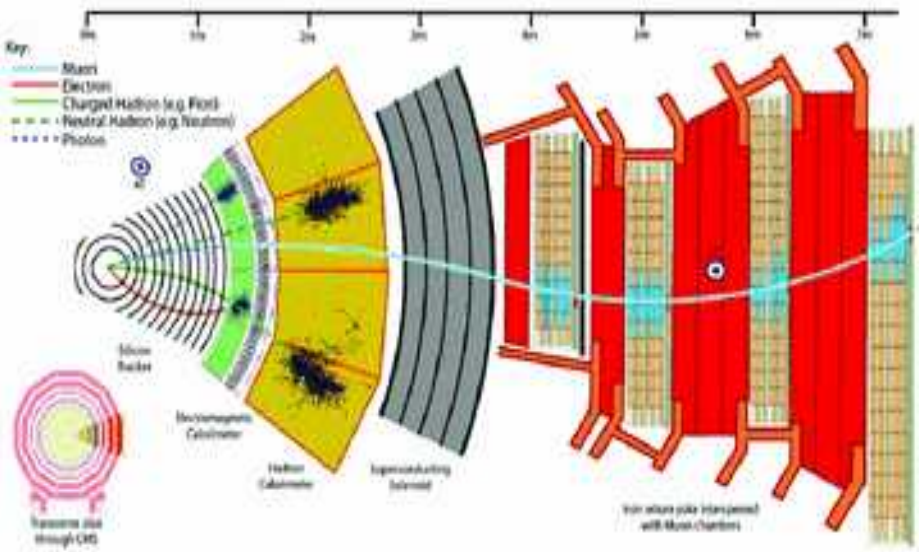
PARTICLES-MATTER INTERACTIONS



Détecteur

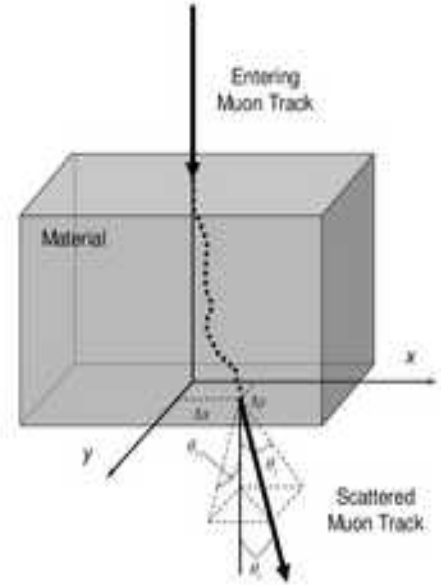


Détecteur



$$\left\langle \frac{dE}{dx} \right\rangle = K z^2 \frac{Z}{A} \frac{1}{\beta^2} \left[\frac{1}{2} \ln \frac{2m_e c^2 \beta^2 \gamma^2 W_{max}}{I^2} - \beta^2 - \frac{\delta(\beta\gamma)}{2} \right]$$

absorption



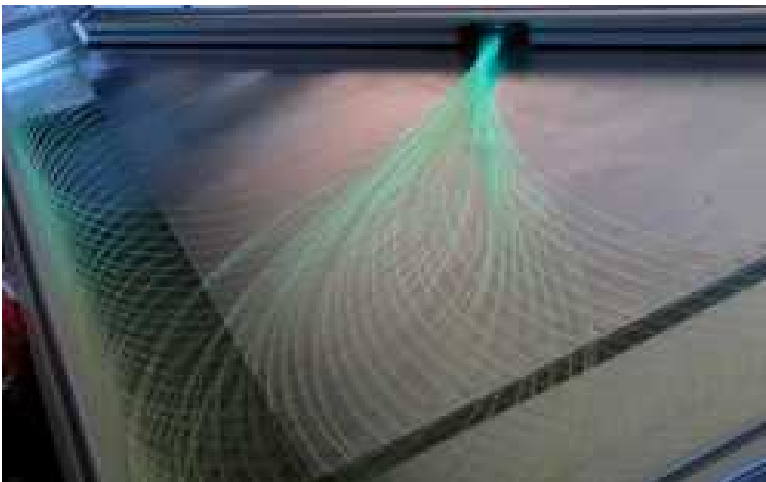
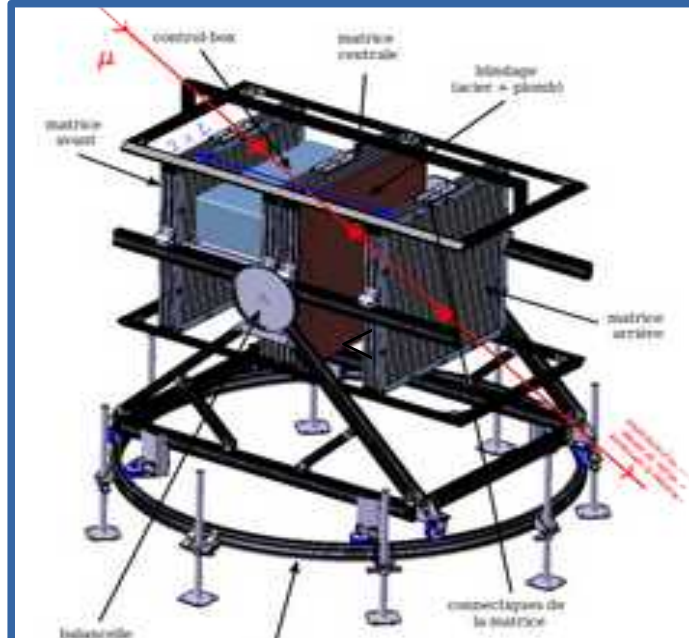
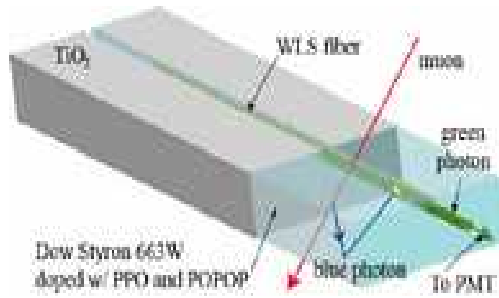
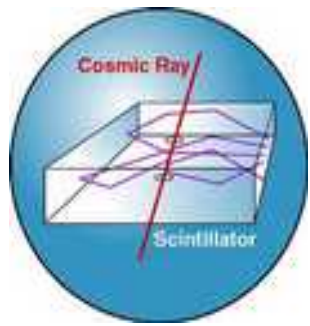
$$\theta_0 = \frac{13.6 \text{ MeV}}{\beta c p} \approx \sqrt{\frac{x}{X_0}} \left[1 + 0.088 \log_{10} \left(\frac{x z^2}{X_0 \beta^2} \right) \right]$$

scattering

$$\varrho(L) \equiv \int_L \rho(\xi) d\xi$$

ϱ = opacity ρ = density

TRACKERS



Scintillators



Emulsions

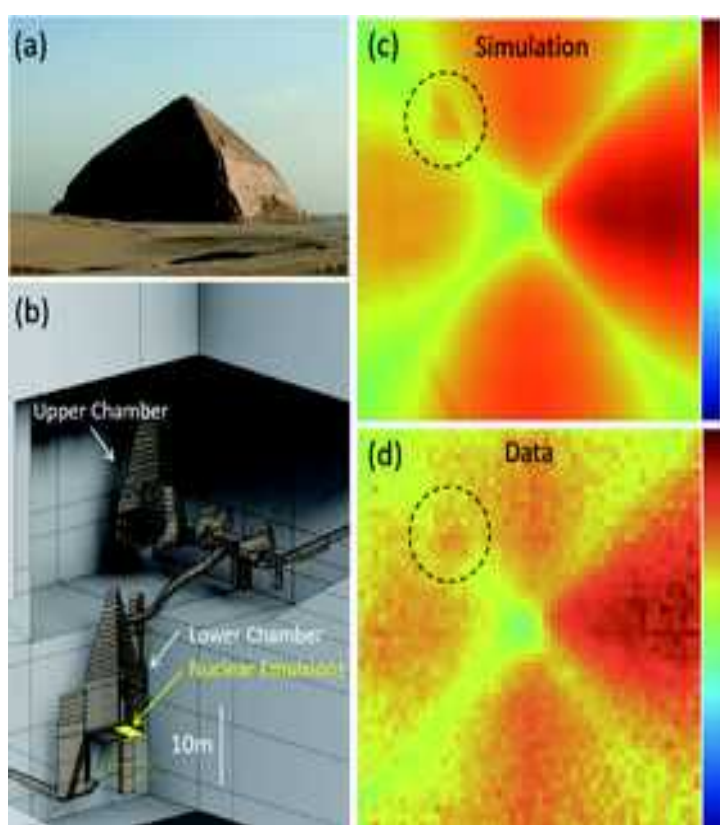


RPC



Micromegas

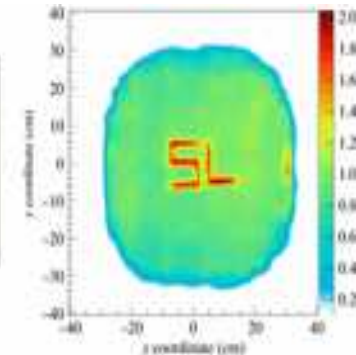
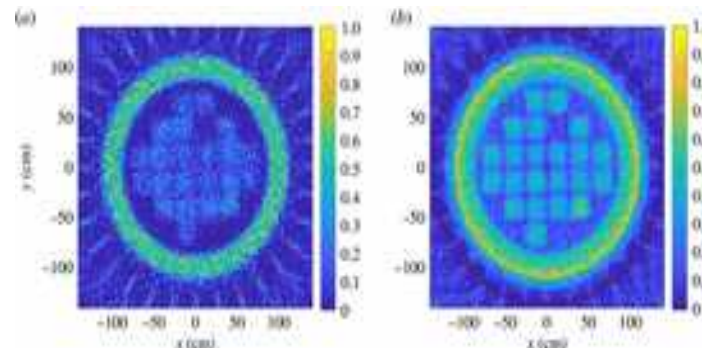
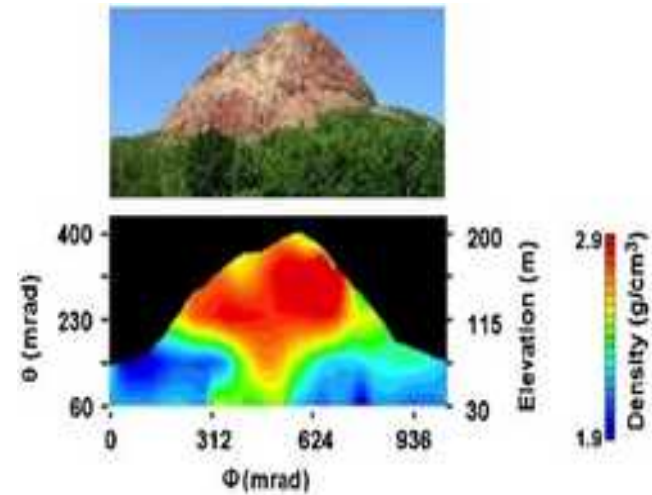
IMAGING METHODS



Détecteur

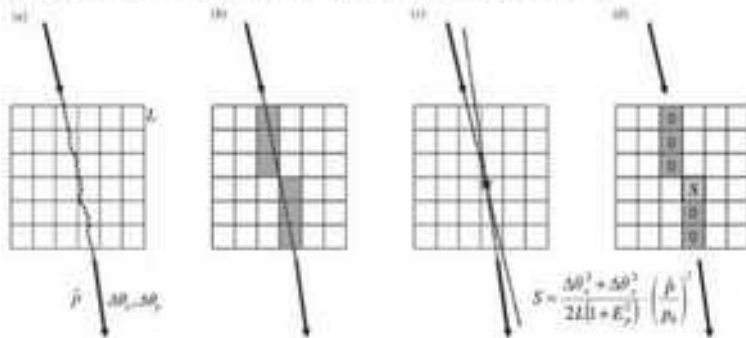
Reconstruction

Images

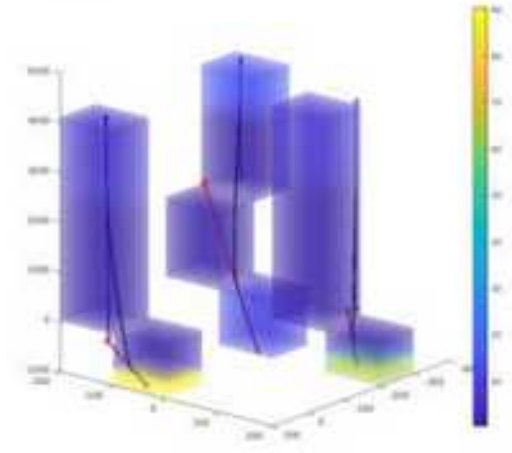
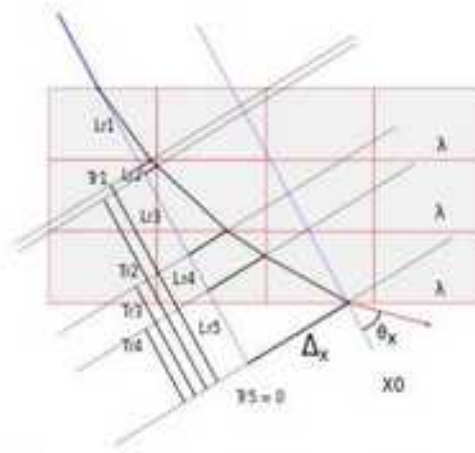


INVERSE PROBLEMS

POCA 3D: Point of Closest-Approach



MLEM: Maximum Likelihood Expectation Maximisation



$$P(D_i | \lambda) = \frac{1}{2\pi |\Sigma_i|^{1/2}} \exp \left(-\frac{1}{2} D_i^T \Sigma_i^{-1} D_i \right)$$

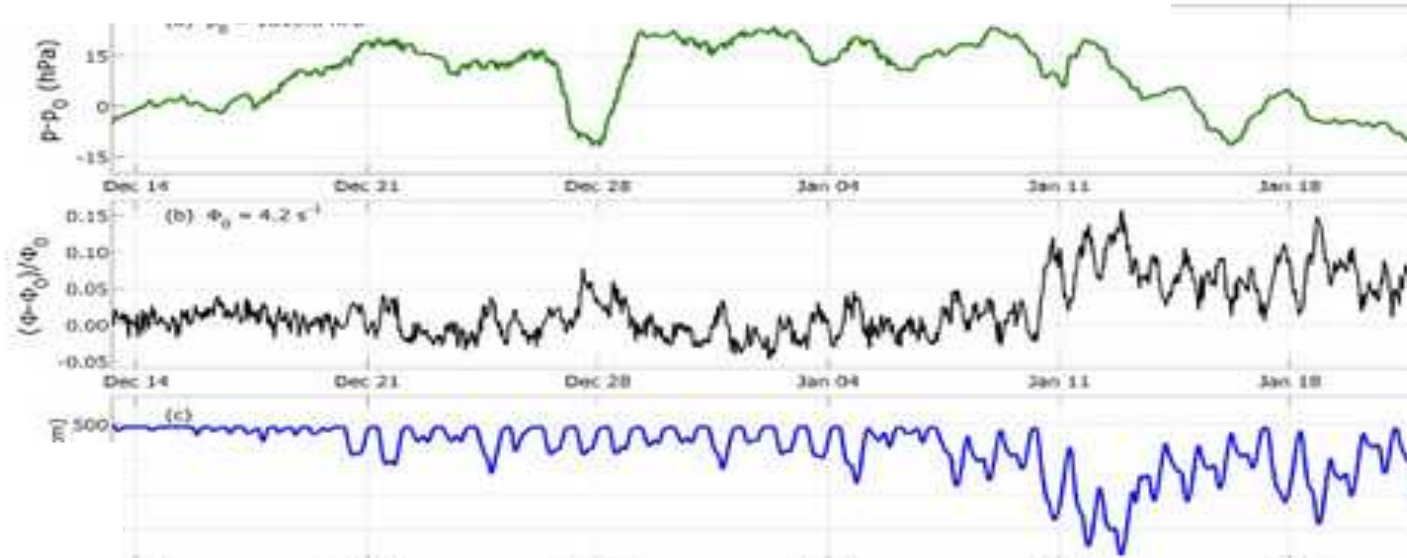
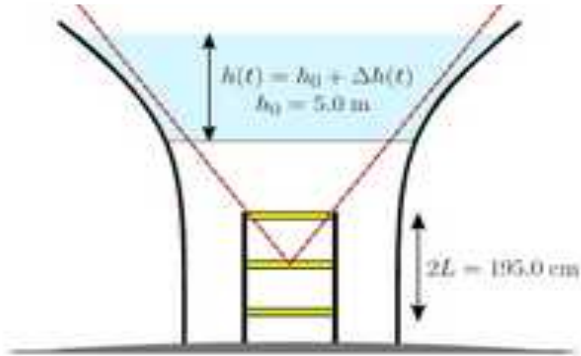
$$P(D_i | \lambda) = \frac{1}{2\pi |\Sigma_i|^{1/2}} \exp \left(-\frac{1}{2} D_i^T \Sigma_i^{-1} D_i \right)$$

$$\Sigma_i = p_{r,i}^2 \sum_{j \leq N} \lambda_j W_{ij}$$

$$W_{ij} = \begin{bmatrix} L_{ij} & L_{ij}^2/2 + L_{ij}T_{ij} \\ L_{ij}^2/2 + L_{ij}T_{ij} & L_{ij}^2/3 + L_{ij}^2T_{ij} + L_{ij}T_{ij}^2 \end{bmatrix}$$

$$\frac{1}{|\Sigma_i|} (\Delta\theta_x^2 v_{xx} - 2\Delta\theta_x \Delta\theta_y v_{xy} + \Delta\theta_y^2 v_{yy})$$

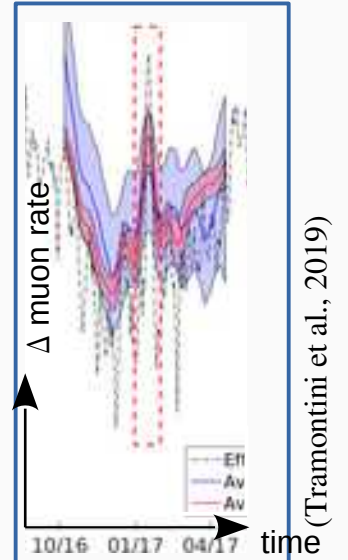
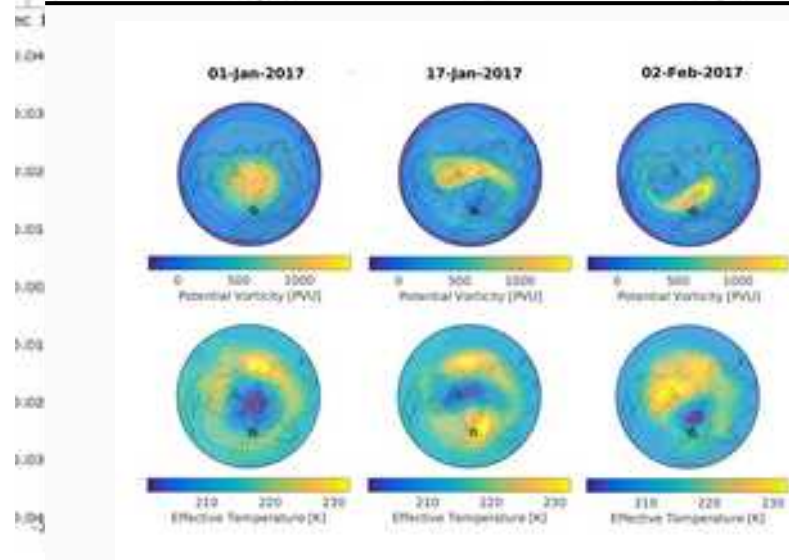
MONITORING METHODS



- ▶ Proof of concept
- ▶ Water tank level monitoring
- ▶ Barometric effects corrections

$$\frac{\Delta R}{\langle R \rangle} = \alpha_T \frac{\Delta T_{\text{eff}}}{\langle T_{\text{eff}} \rangle} + \beta_P (p - \langle p \rangle)$$

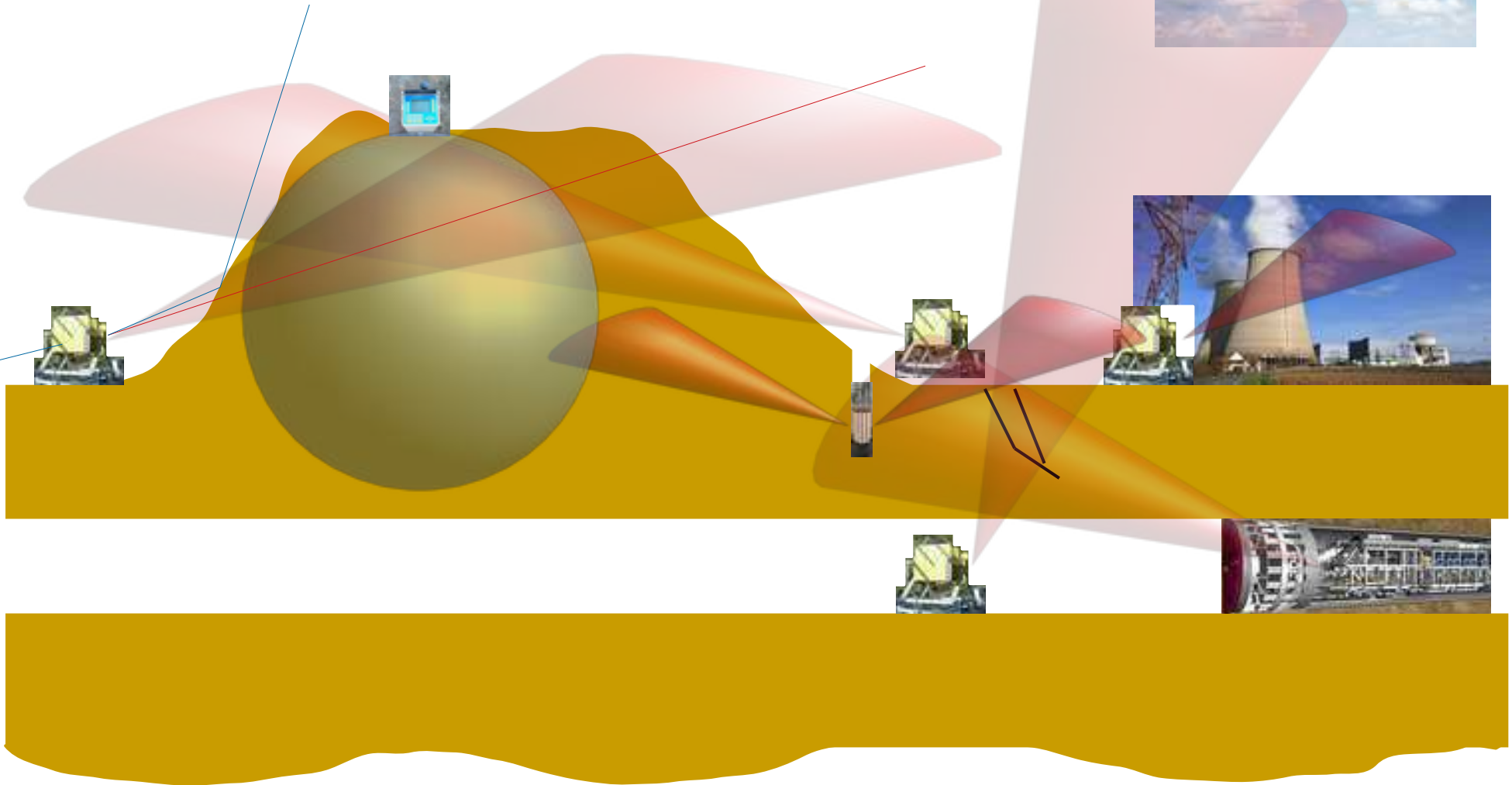
- ▶ Geomagnetic effects etc
- ▶ Application to the Sudden Stratospheric Warming (SSW) observation



(Tramontini et al., 2019)

Field muography use cases

1. "radio"-like structural imaging & monitoring
2. "scanner"-like structural imaging & monitoring
3. joined analysis with geotechnics
4. static underground imaging (+atmosphere physics)
5. dynamic underground imaging
6. borehole applications



Muography use cases overview

Muography = transmission/scattering imaging technique → sensitive to (scattering) density + Z/A

Geosciences



- Volcanology
- Geology
- Hydrology
- Atmosphere physics
- CR physics
- ...

Archaeology

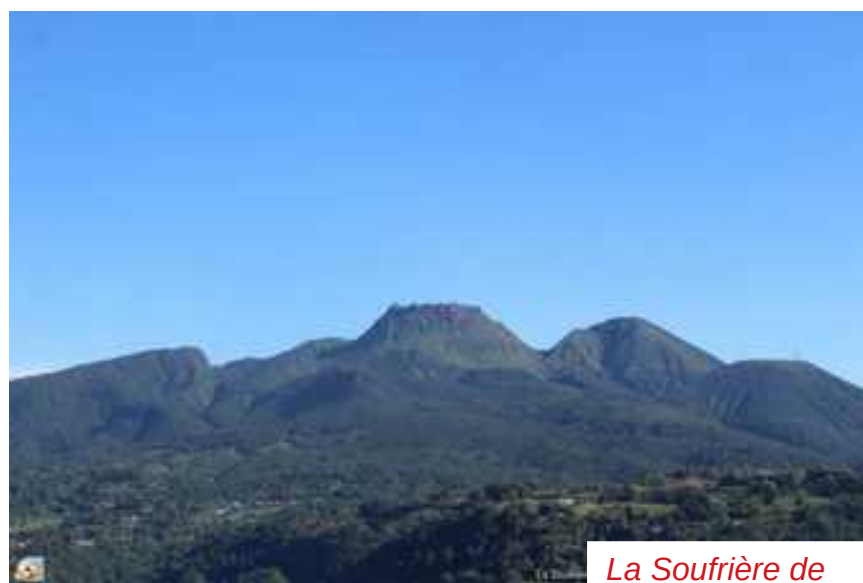


- Pyramids
- Tumulus
- Anthropic structures
- Ruins
- ...

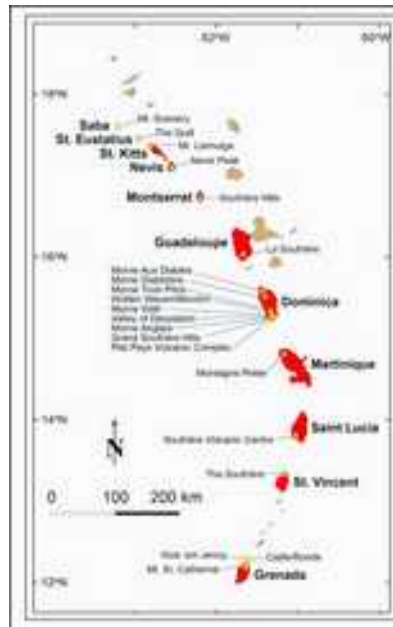
Industrial controls



- Non invasive controls
- Nuclear cycle production
- Civil engineering
- Tunnel boring machines
- Prospection & mining
- ...



La Soufrière de Guadeloupe



Etna

Volcanoes



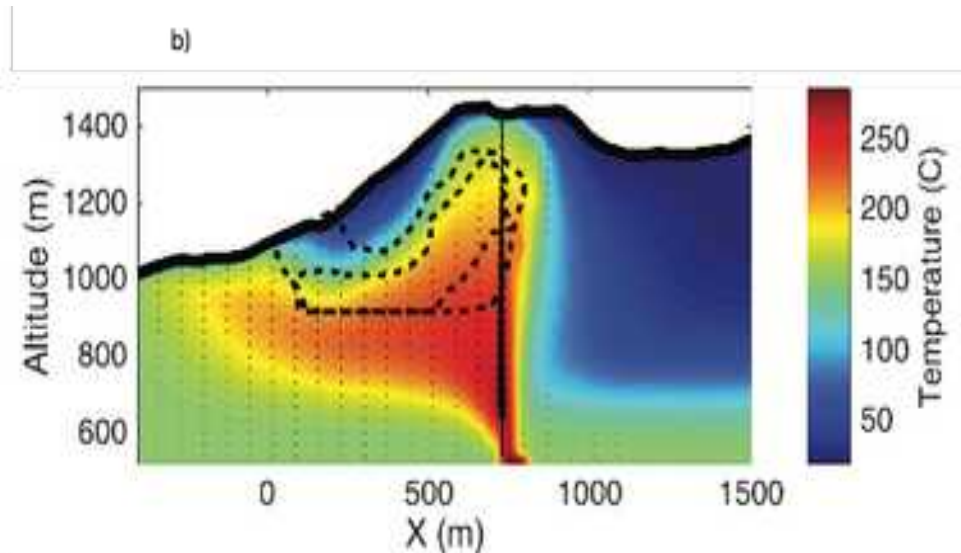
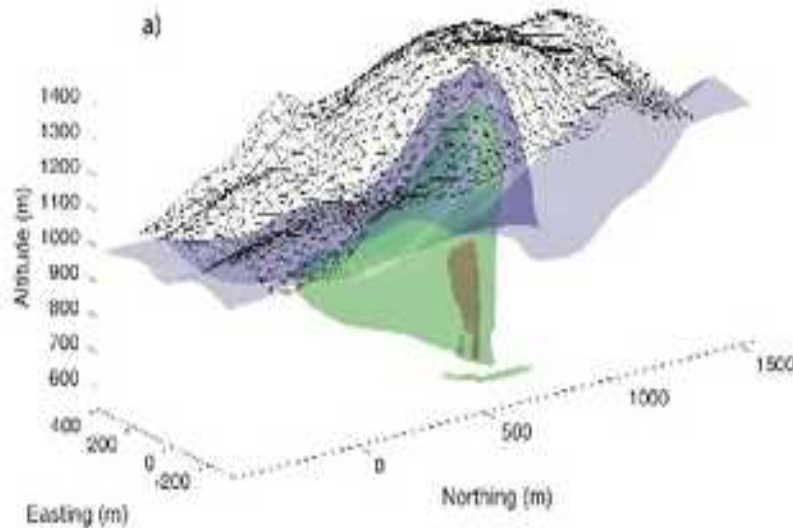
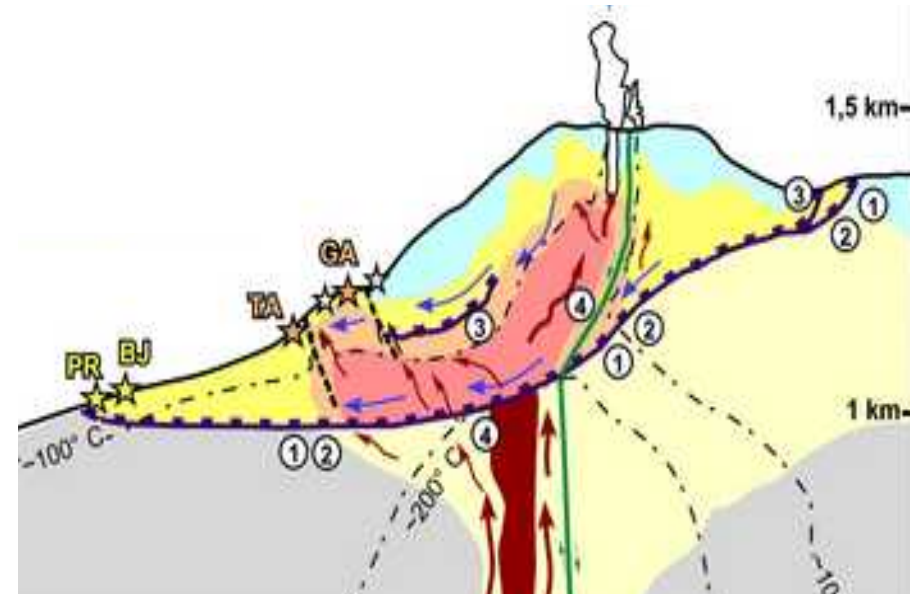
Snæfellsjökull



Mayon

La Soufrière hydrothermal systems

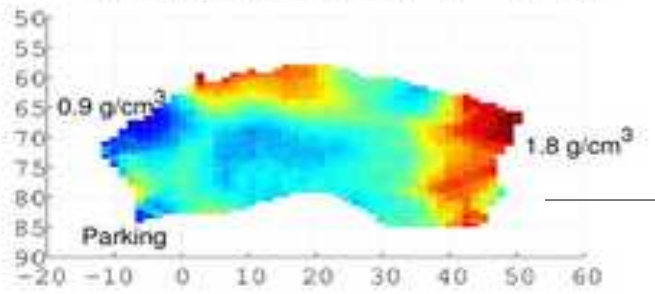
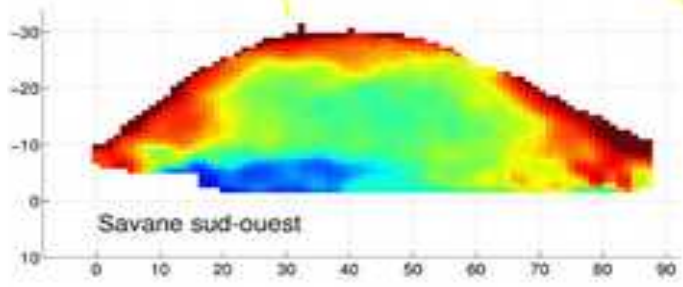
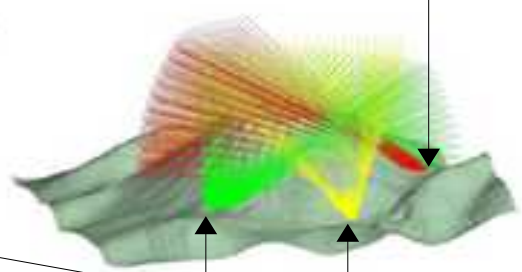
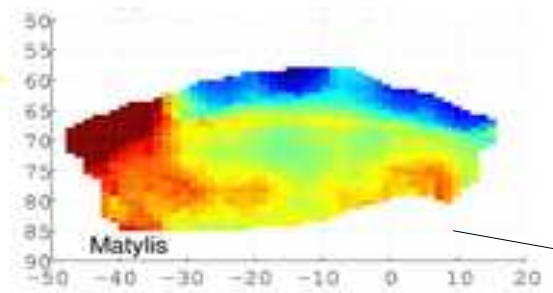
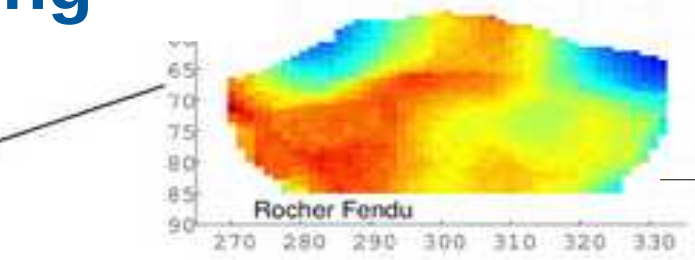
- Volcano hydrothermal systems are at the core of unpredictable volcanic hazards
- Complex interplay between internal and external forcing
- Classical geophysics provide limited information on spatio-temporal dynamics
- Need for techniques that can track in space and time the internal state of the system to constrain numerical models



La Soufrière “muon station”

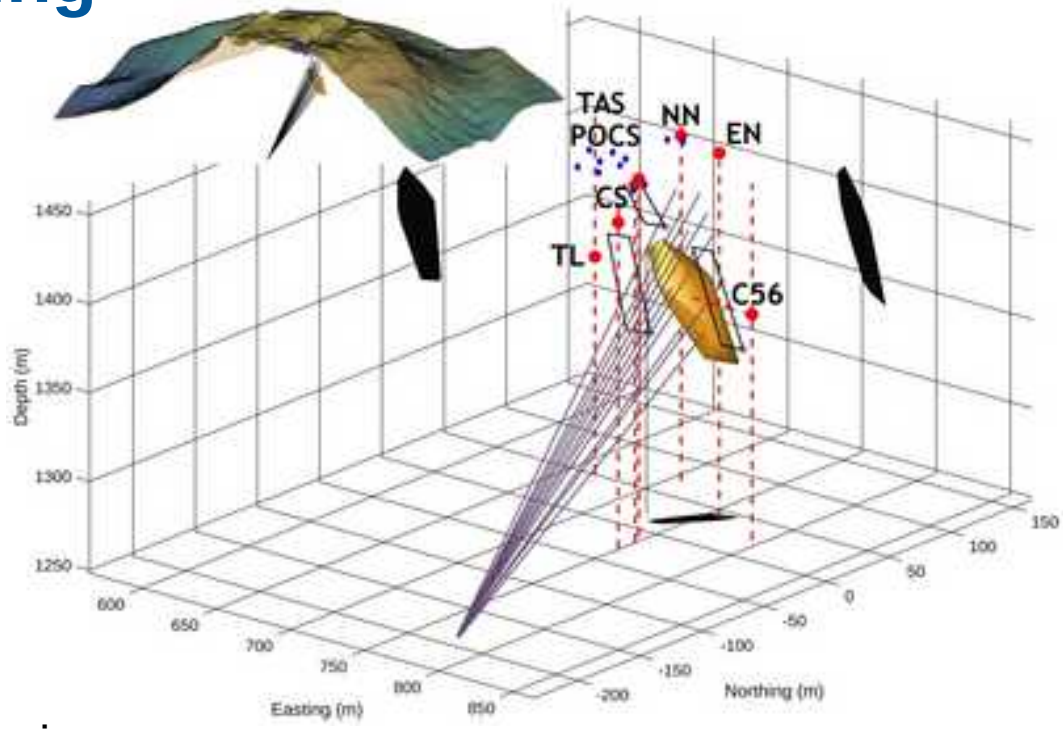
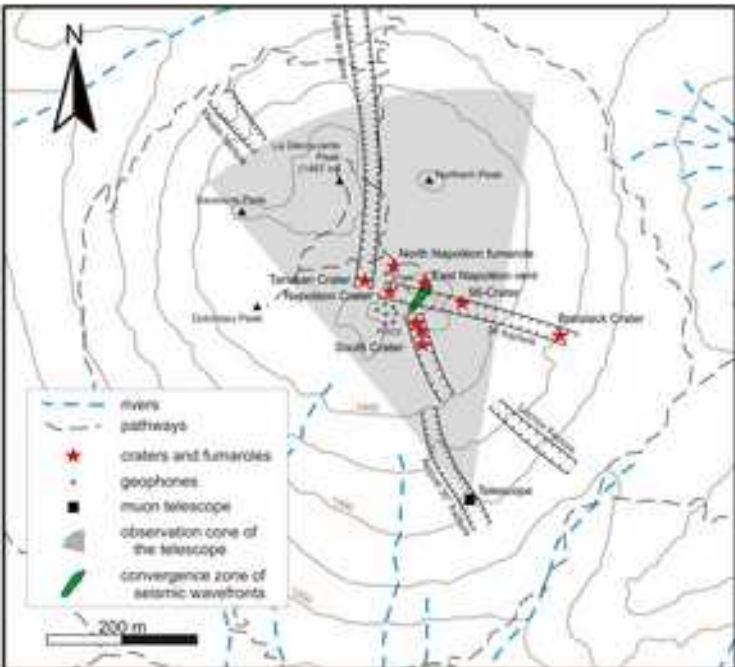


Imaging & monitoring

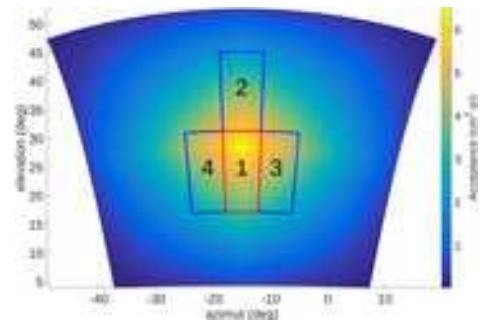
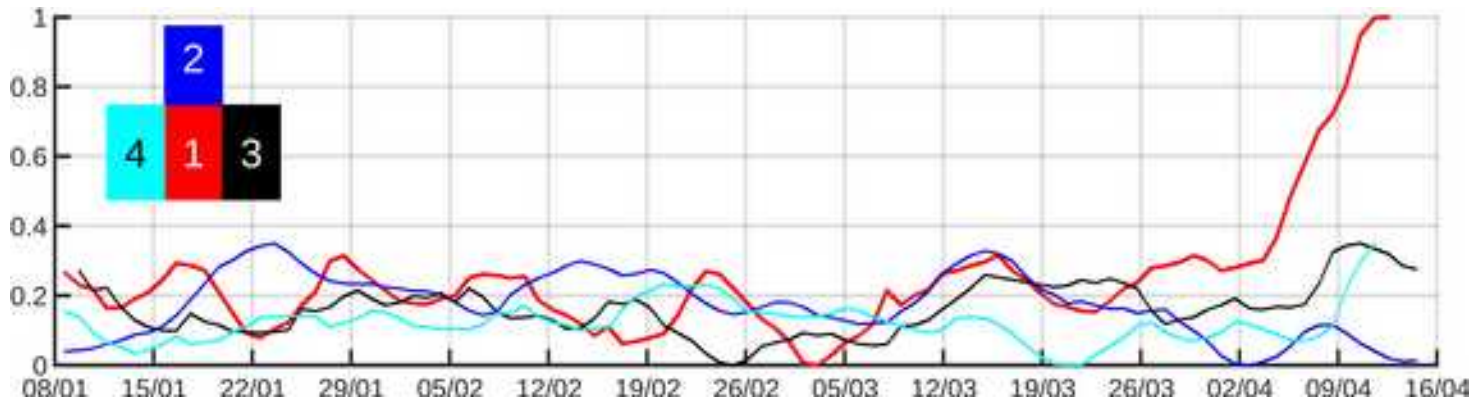


The largest muons station in the world (6 detectors running)

Sismo-muon joint monitoring

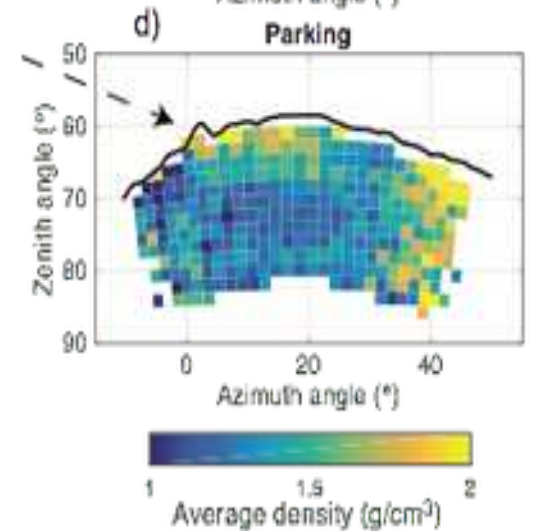
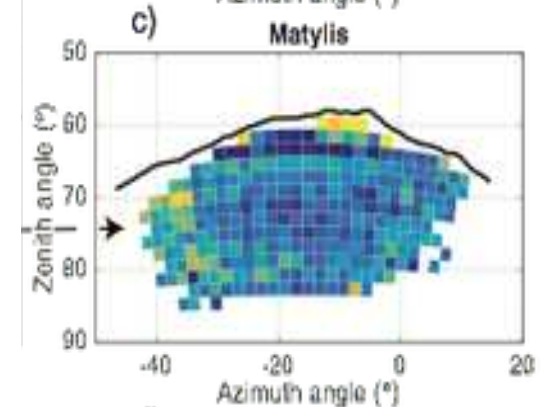
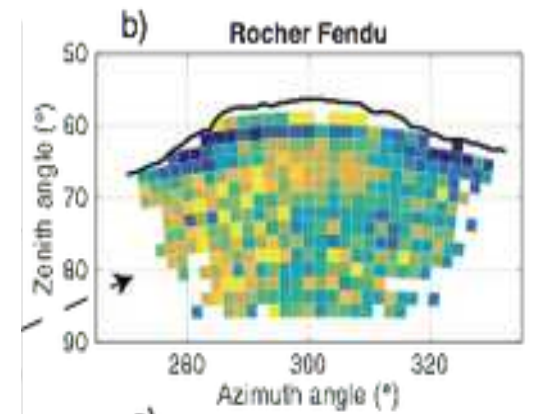
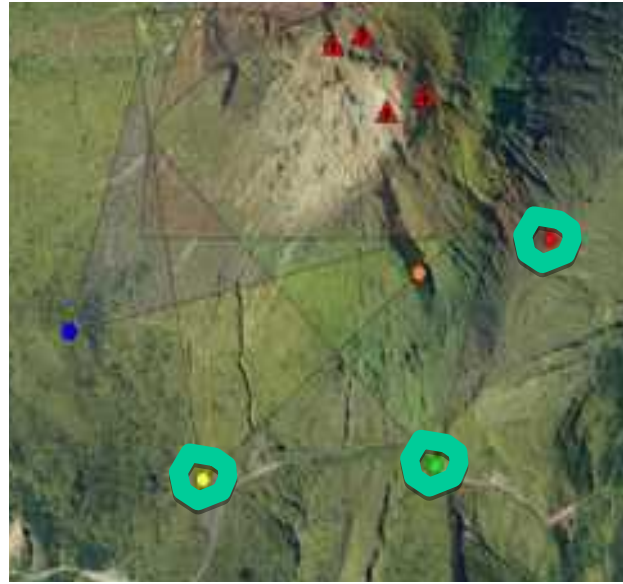
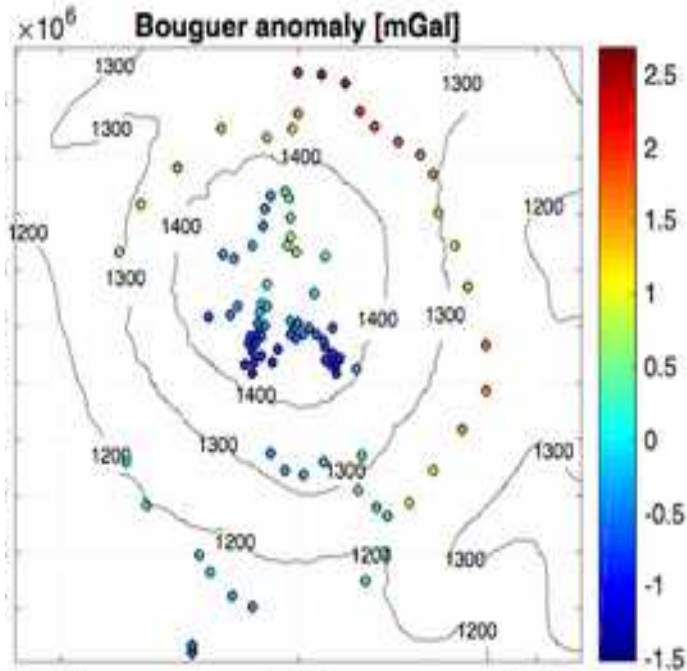


Global analysis of muon and seismic monitoring



Abrupt changes of hydrothermal activity in a lava dome detected by combined seismic and muon monitoring : *Le Gonidec, J.-Y. et al. Scientific Reports 2019*

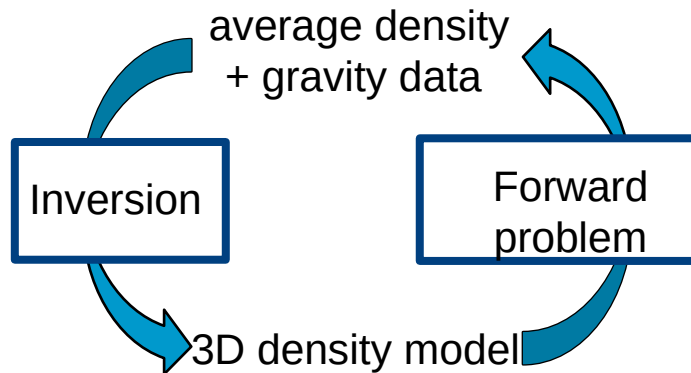
3-D gravi-muon joint inversion



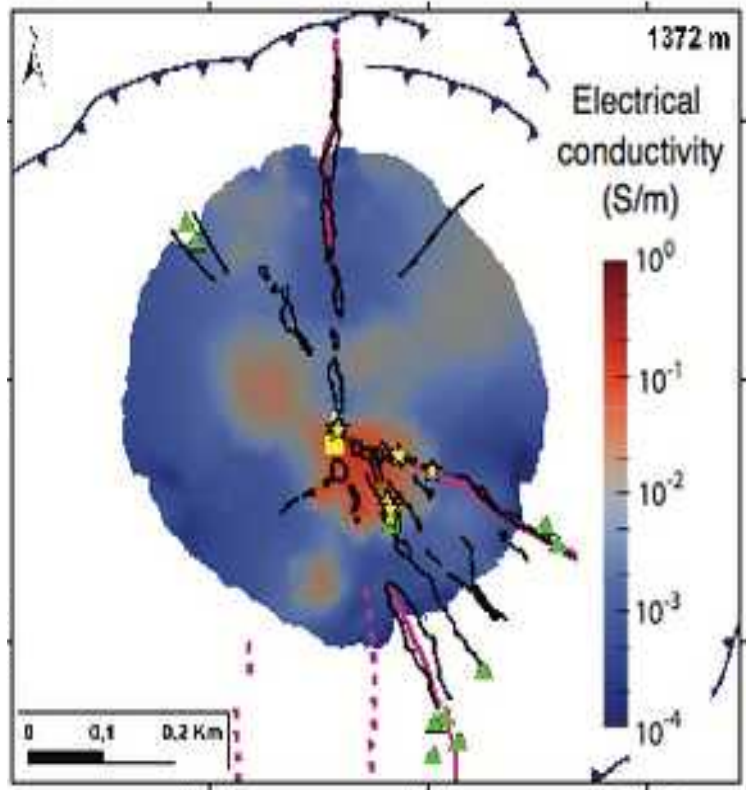
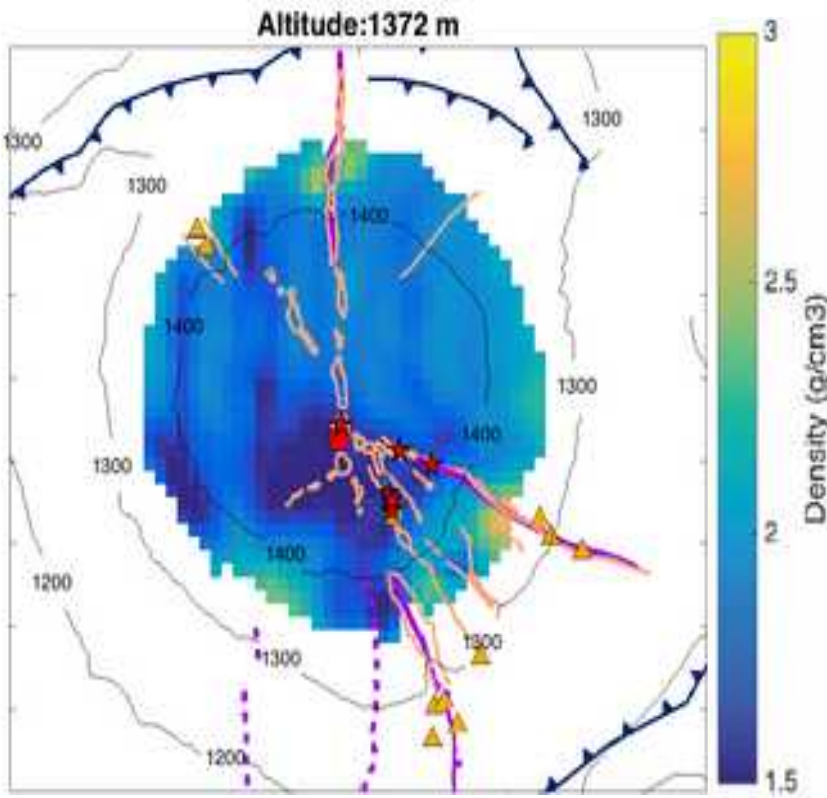
$$G \begin{bmatrix} \rho_\mu \\ \Delta\rho \end{bmatrix} = \begin{bmatrix} G_g \\ G_\mu \end{bmatrix} \begin{bmatrix} \rho_\mu \\ \Delta\rho \end{bmatrix} = \begin{bmatrix} \mathbf{d}_g \\ \mathbf{d}_\mu \end{bmatrix} = \mathbf{d}$$

$$\phi(\mathbf{m}) = (\mathbf{d} - G\mathbf{m})^T C_d^{-1} (\mathbf{d} - G\mathbf{m}) + \epsilon^2 (\mathbf{m} - \mathbf{m}_{\text{prior}})^T C_\rho^{-1} (\mathbf{m} - \mathbf{m}_{\text{prior}})$$

Smoothing \swarrow \searrow Damping \swarrow Matrix scaling



Horizontal slices of density and electrical conductivity models



(Rosas-Carbajal et al., 2016, 2017)

LIDENBROCK & SNAEFELLSJOKULL



T.AVGITAS¹, S.BARSOTTI³, G.BJÖRNSSON⁴, J.BJÖRNSSON⁵, B.CARLUS^{1,2}, A.CHEVALIER²,
A.COHU¹, J.-C.IANIGRO^{1,2}, J. MARTEAU^{1,2}, J.-L.MONTORIO¹, C.MÜLLER⁶, C.PICHOL-THIEVEND²

1 – INSTITUT DE PHYSIQUE DES 2 INFINIS DE LYON (IP2I), UNIVERSITÉ LYON-1, CNRS-IN2P3 (UMR5822)

2 – MUODIM, 31 RUE SAINT-MAXIMIN, 69003 LYON

3 – IMO, REYKJAVIK

4 – WARM ARCTIC, SKJOLBRAUT 22, IS-200 KOPAVOGUR, ICELAND

5 – SNAEFELLS NATIONAL PARK

6 – [HTTPS://CAROLMULLER.FR/](https://carolmuller.fr/)

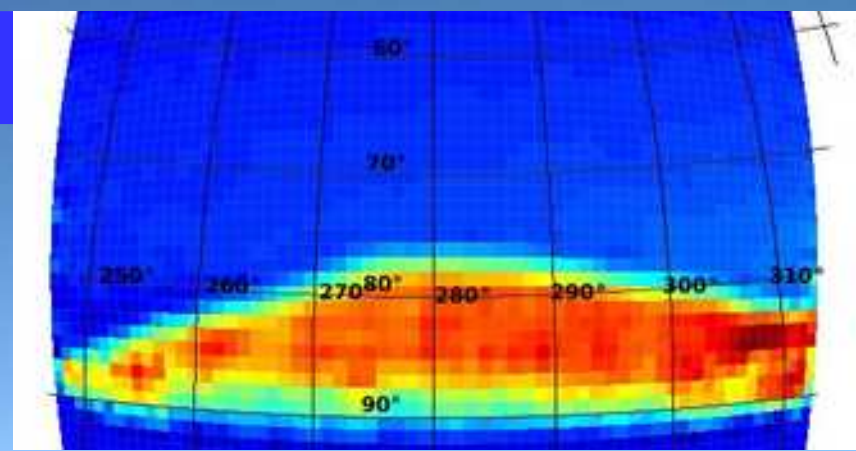
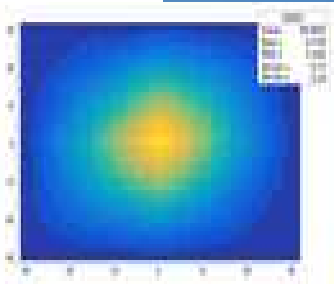
J. MARTEAU^{1,2} (MARTEAU@IN2P3.FR & JACQUES.MARTEAU@MUODIM.COM)



Detector mounting and assembly



First lights

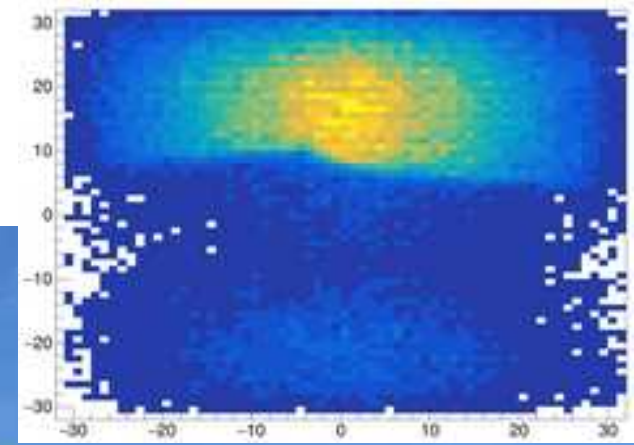


open sky



tomographic mode

Second run





Nuclear evaporator



TBM



Silos

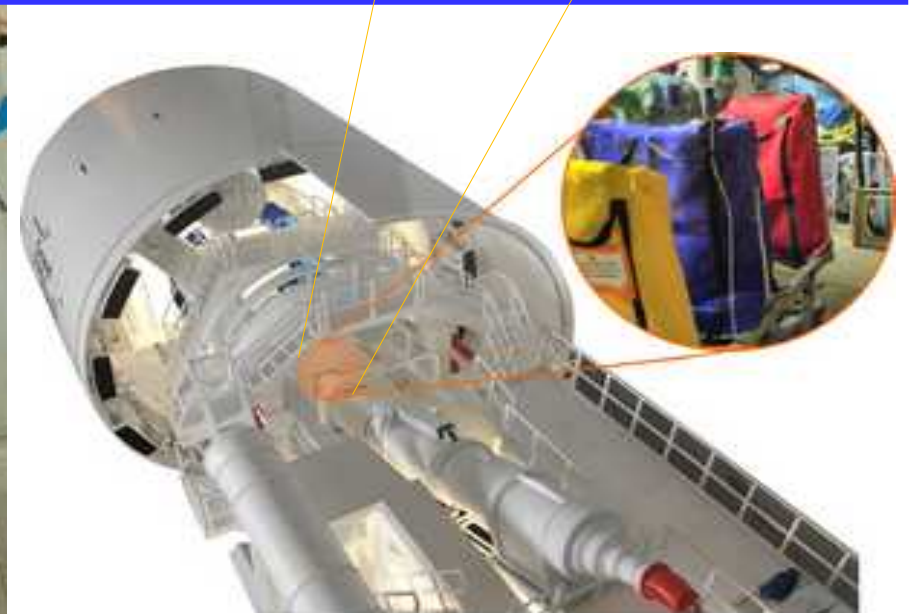


Blast furnace

Geotechnics

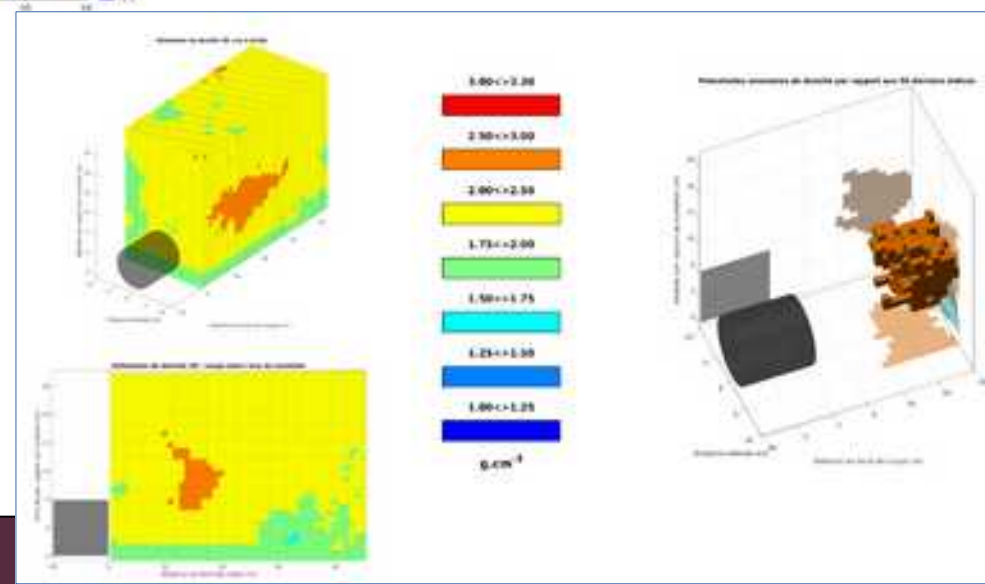
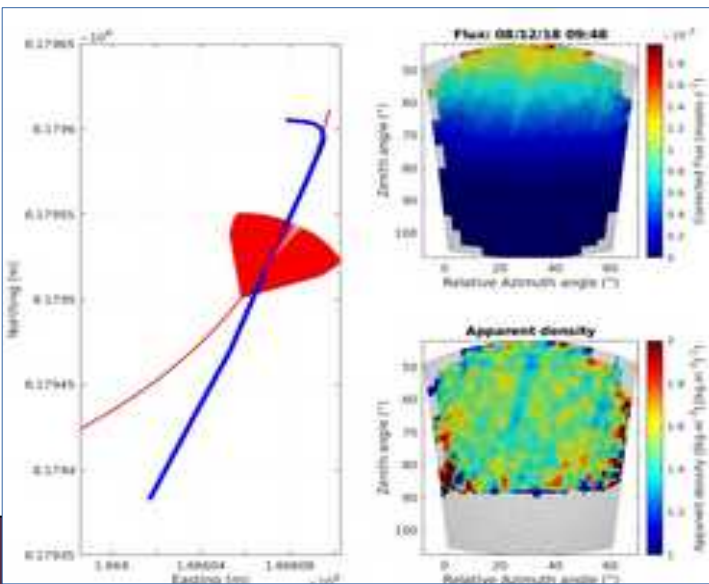
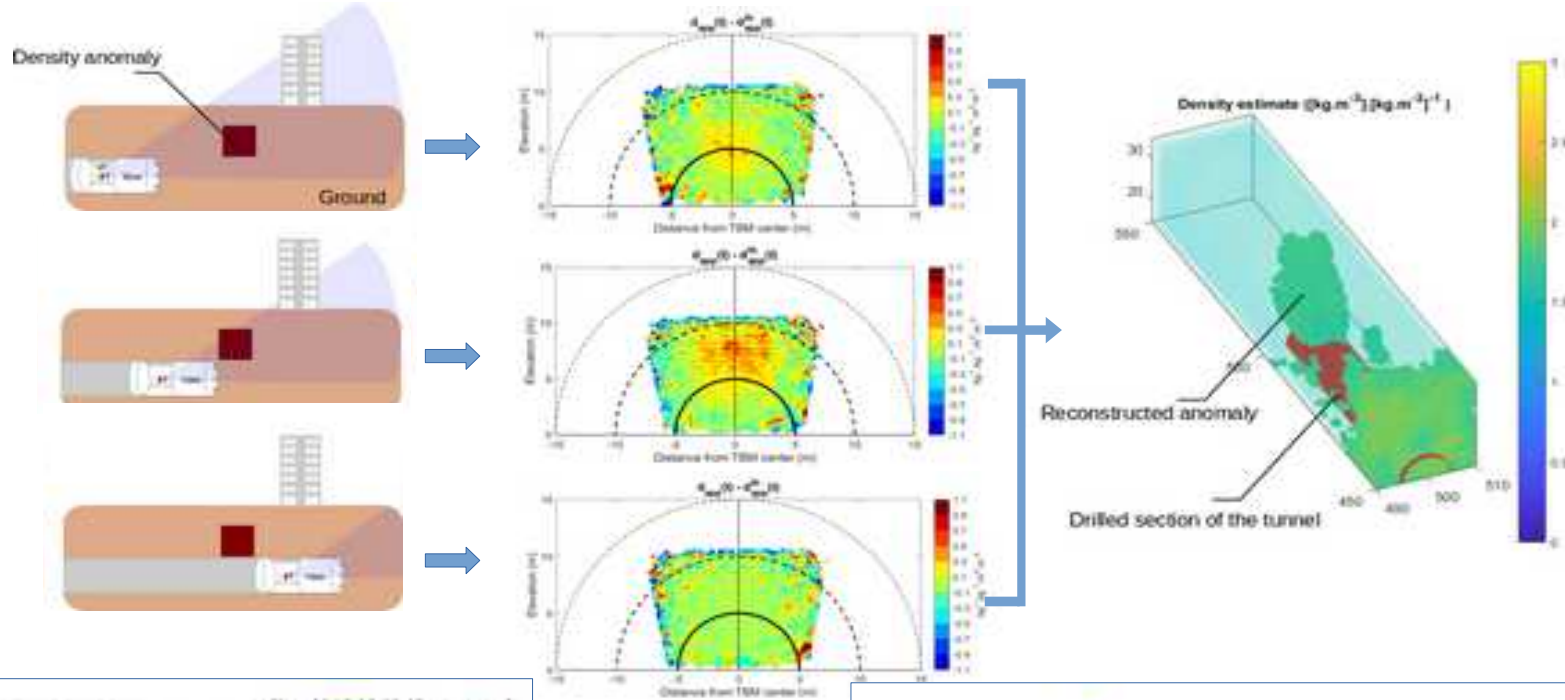


Application to Tunnel Boring machines



Confidentiel

Measurements Principles & Density anomaly detection





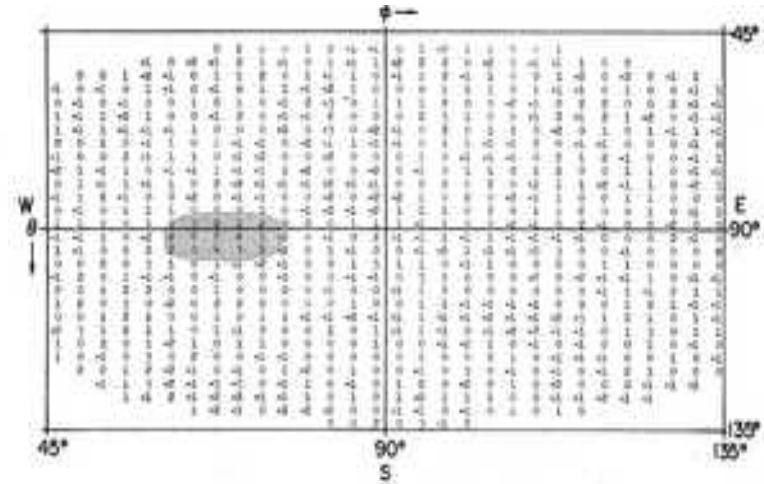
Great pyramids

Search for Hidden Chambers in the Pyramids

The structure of the Second Pyramid of Giza
is determined by cosmic-ray absorption.

Luis W. Alvarez, Jared A. Anderson, F. El Bedwei,
James Burkhard, Ahmed Fakhry, Adib Girgis, Amir Gonod,
Fikhy Hassan, Dennis Iverson, Gerald Lynch, Zenab Miligy,
Ali Hilmy Mounsa, Mohammed-Sharkawi, Lauren Yablino

L. Alvarez paper



Archaeology



Greek tumulus



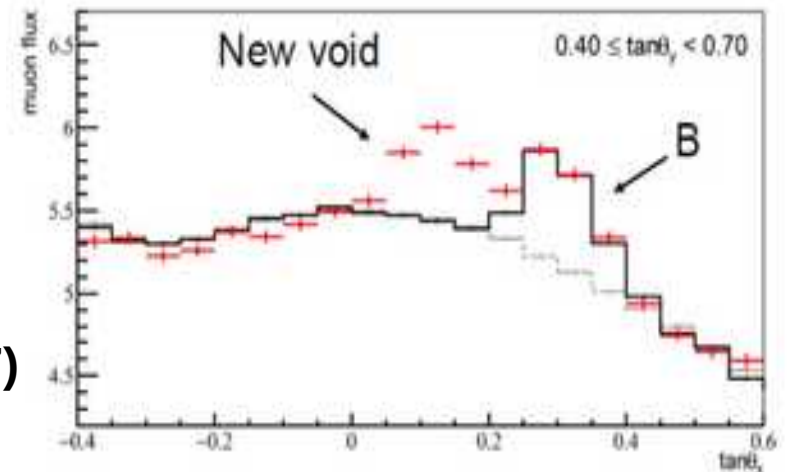
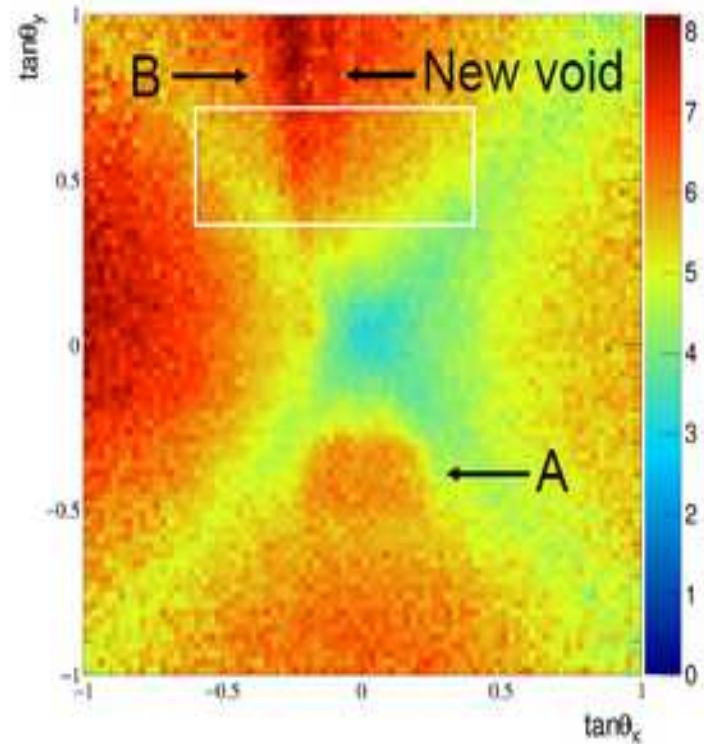
ArchéMuons

The ScanPyramids project

Discovery of a big void in Khufu's Pyramid by observation of cosmic-ray muons



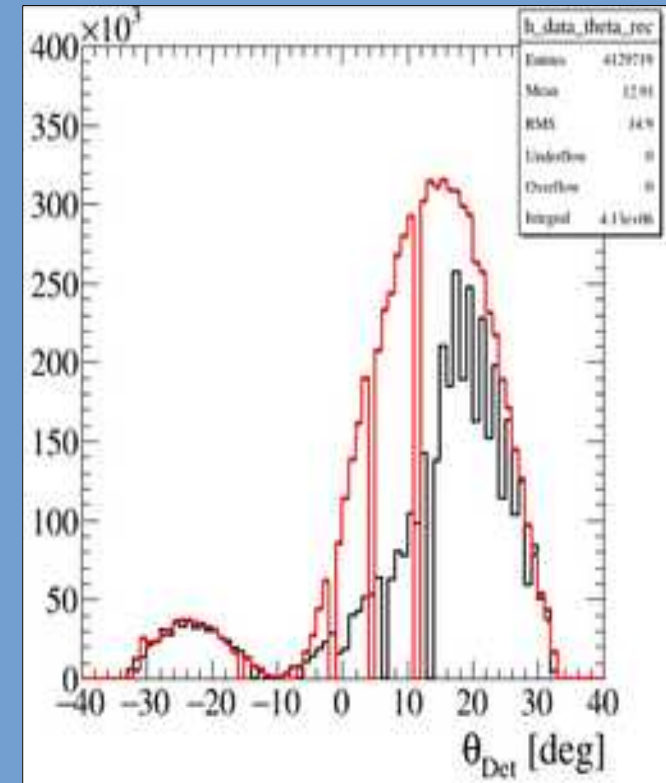
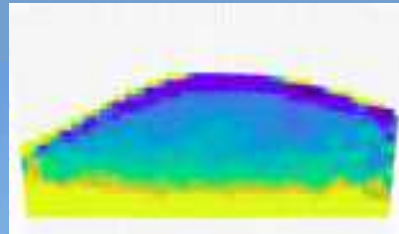
(388 | Nature | VOL 552 | 21/28 DECEMBER 2017)



The Apollonia tumulus

Challenges :

- Looking for an object with similar density as the surrounding materials $\rho \sim 2.3 \text{ gr/cm}^3$ for dirt and 2.5 gr/cm^3 for marble !
- If any monument, it must be at the horizon level. Very low number of muons, wait a LONG time !
- Muons must cross a lot of dirt. Need high energy muons, their number is even less !



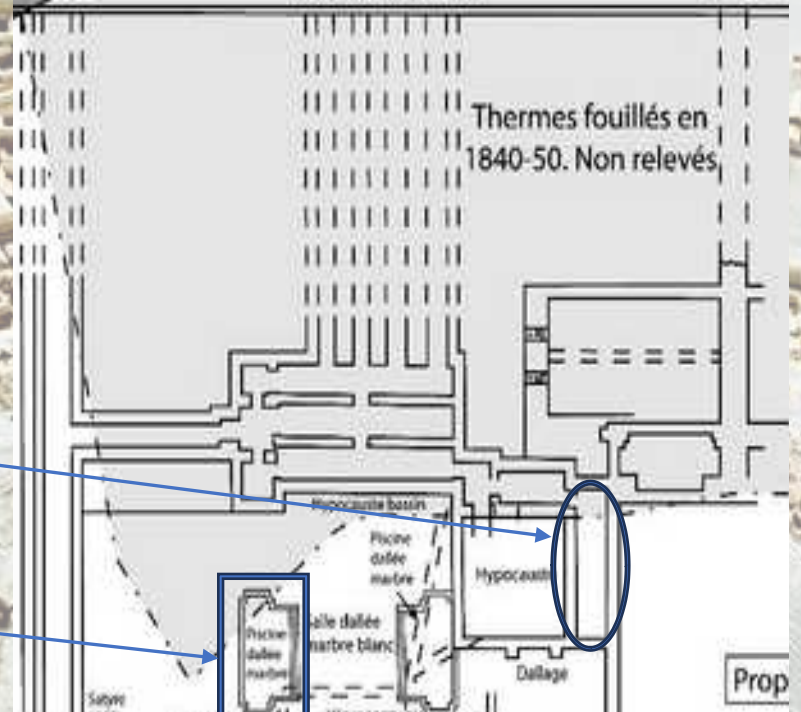
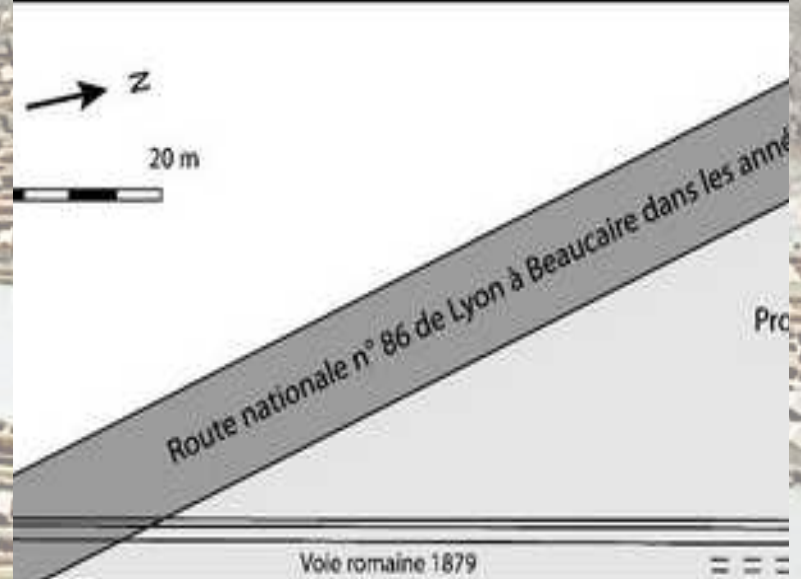
ArchéMuons

- Muon Tomography in controlled/confined environment
- Combine/Compare results with geophysical surveys:
 - ✓ ERT
 - ✓ Gravimetry
 - ✓ Seismometry
- Prospect of archaeological discovery in the “Palais du Miroir”

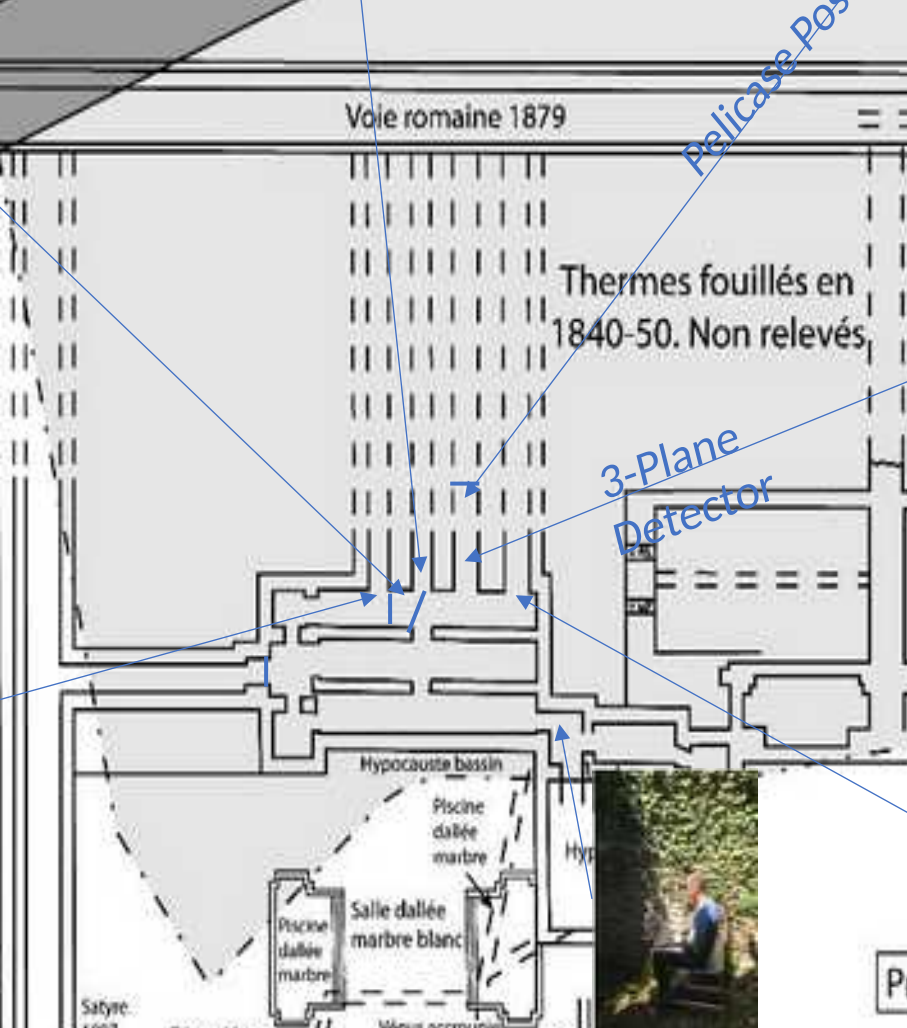
Vienne & St-Romain en Gal



Palais du Miroir – Overground

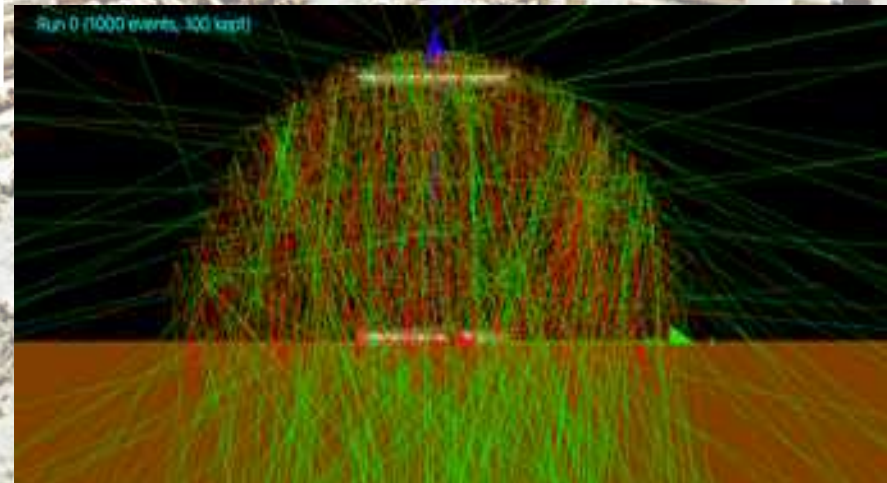
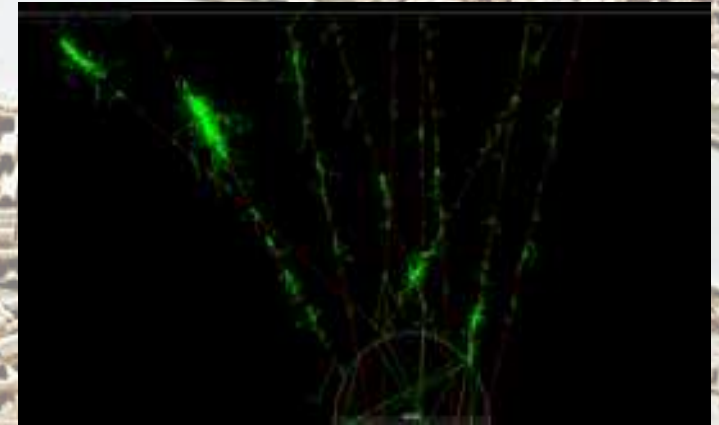
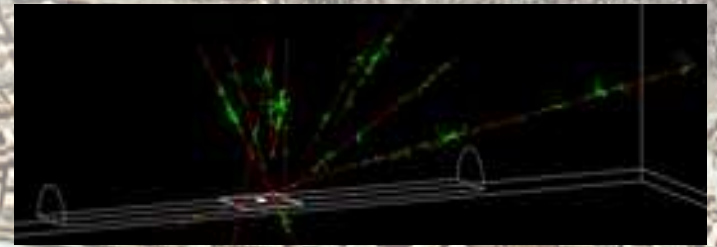


Palais du Miroir – Underground



1840-1850 - Palais du Miroir - Excavation
Plan of the excavated thermes (baths) and the
underground passage. The plan is based on
the archaeological excavations of the
19th century.

MC simulation



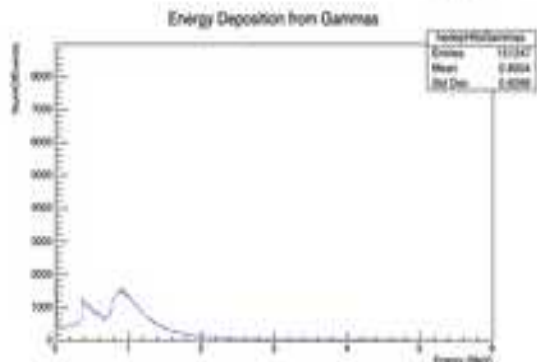
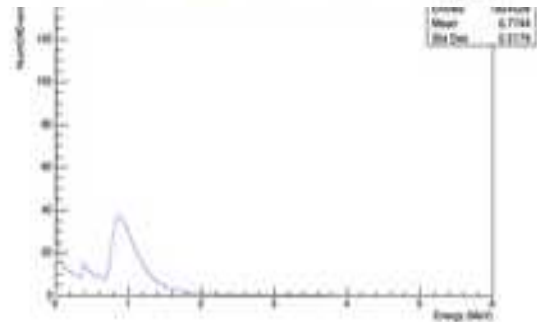
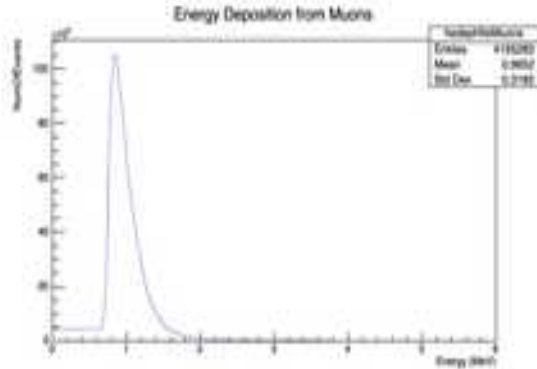
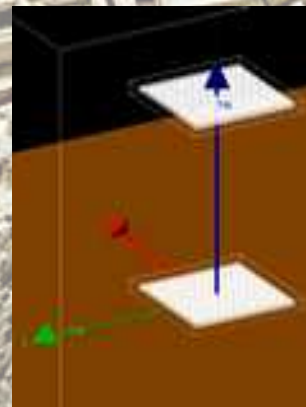
No Cuts

events with hits: 1993708
Events with 2 fold Coincidences: 351286
2-fold Coincidences with muon: 323597
2-fold Coincidences From Muons: 182544

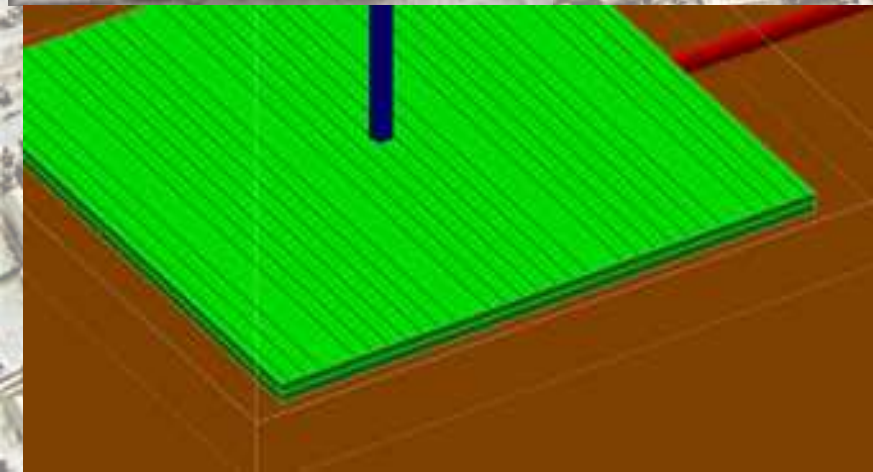
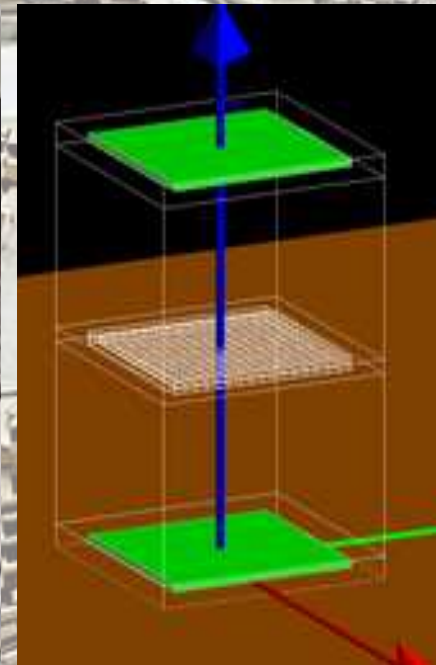
Energy Deposition > 0.6 MeV

events with hits: 1526250
Events with 2 fold Coincidences: 273770
2-fold Coincidences with muon: 272918
2-fold Coincidences From Muons: 173913

Preliminary Finding Shows
2-fold Coincidence are
64% actual muons
36% Muon + other particle



Detector development



Saint-Gobain



ref. Luxium
Solutions

BC-416
203 cm X 63 cm X 5 mm

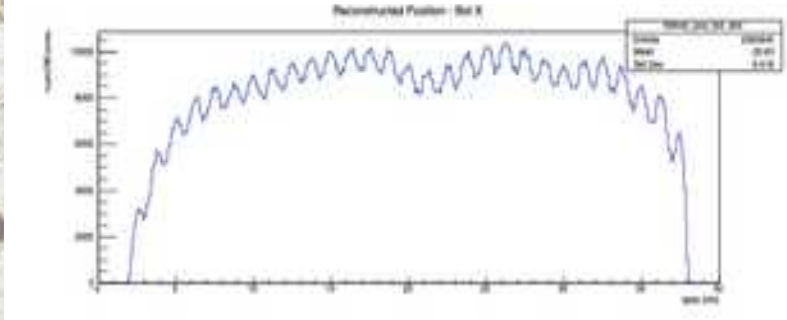
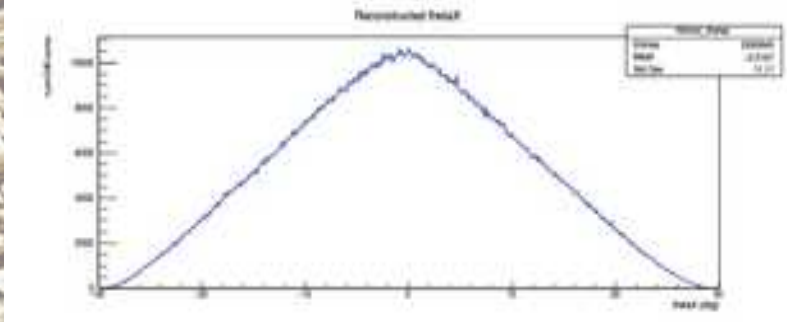
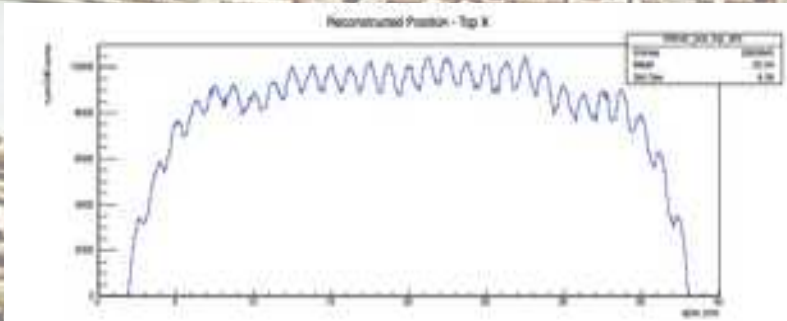
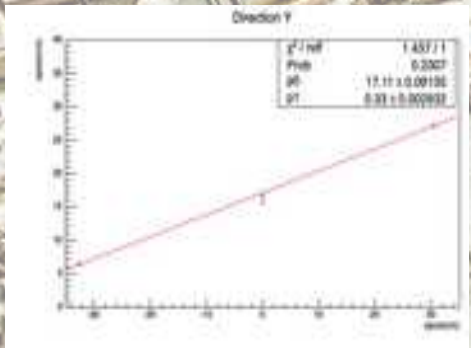
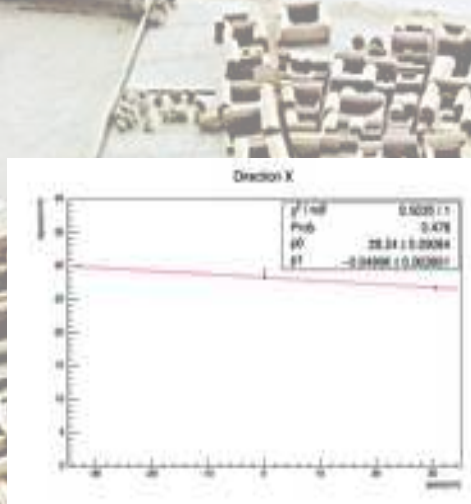
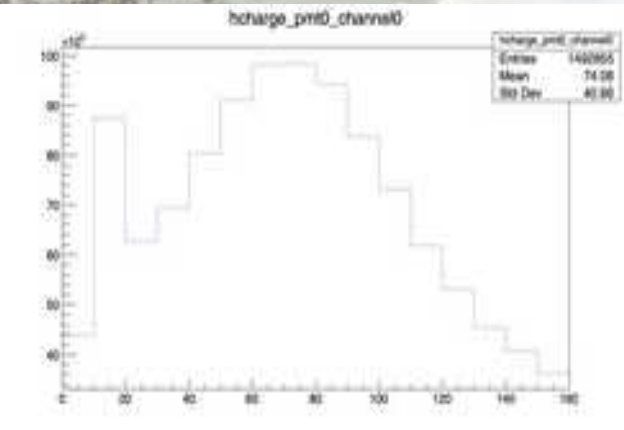
Detection: Alphas, betas,
charged particles, cosmic rays,
Muons, protons

Large Area & Economy

Track Reconstruction from charge deposit

Gold Event Rates:

- (1) $12.8 * 10^{-3}$ Hz
- (2) $8.1 * 10^{-3}$ Hz
- (3) $4.5 * 10^{-3}$ Hz
- (4) $8.4 * 10^{-3}$ Hz

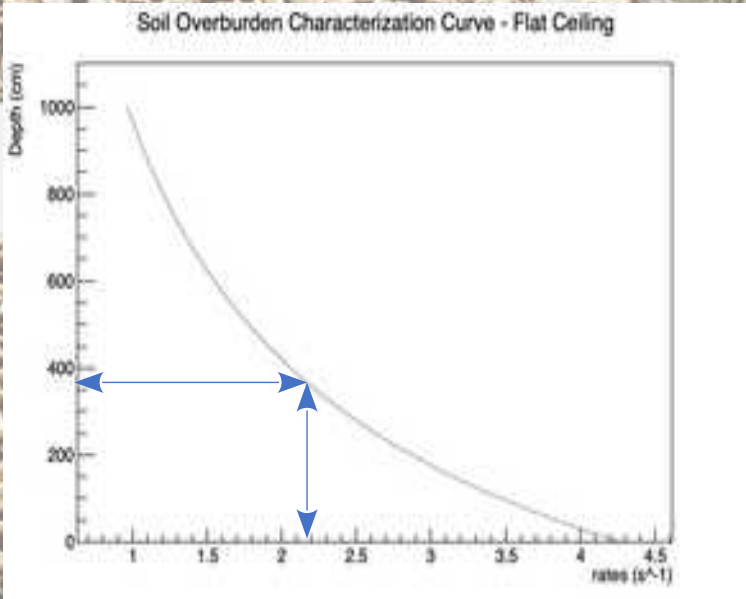
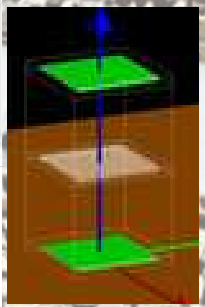
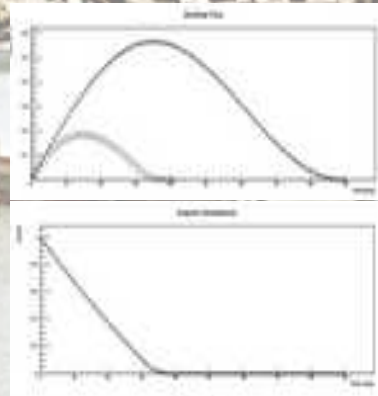
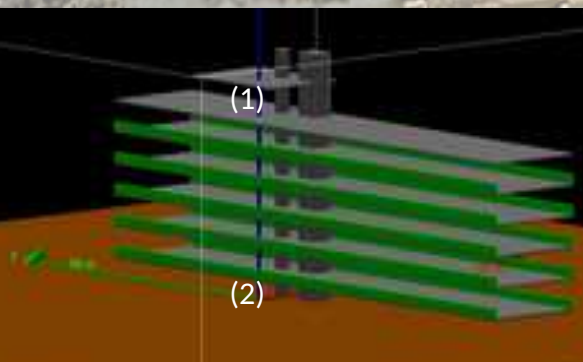


Charge cut:

Extreme plane channels: 30 ADC
Middle plane channels: 25 ADC

- Events that did not give charge on the fibers that are closest to the borders for the extreme panels.
- Events that gave one pair of (x,y) hits for the middle detector
- Exclude events that have position error = 0. This means that the multiplicity for the extreme panels is above 1.

Overburden Thickness Calculation



Detector Efficiency Calculation

Theoretical Rates:

- (1) - 4.120 s^{-1}
- (2) - 3.175 s^{-1}

Experimental Rates:

- (1) - $0.637 \pm 0.0021 \text{ s}^{-1}$
- (2) - $0.480 \pm 0.0027 \text{ s}^{-1}$

Efficiency:

- (3) - 0.1546 ± 0.0005
- (4) - 0.1512 ± 0.0009

Experimental rate inside the Cavity

- 1st Run: $0.3381 \pm 0.0007 \text{ s}^{-1}$
- 2nd Run: $0.3384 \pm 0.0009 \text{ s}^{-1}$
- 3rd Run: $0.3209 \pm 0.0008 \text{ s}^{-1}$

$\langle \text{Rate} \rangle = 0.3326 \pm 0.0005 \text{ s}^{-1}$

Divide by efficiency

$\text{Rate} = 2.182 \pm 0.003 \text{ s}^{-1}$

Overburden Characterization Curves

Two Geometries for the overburden.

- (a) Rectangular &
- (b) Rectangular with Semispherical Cavity

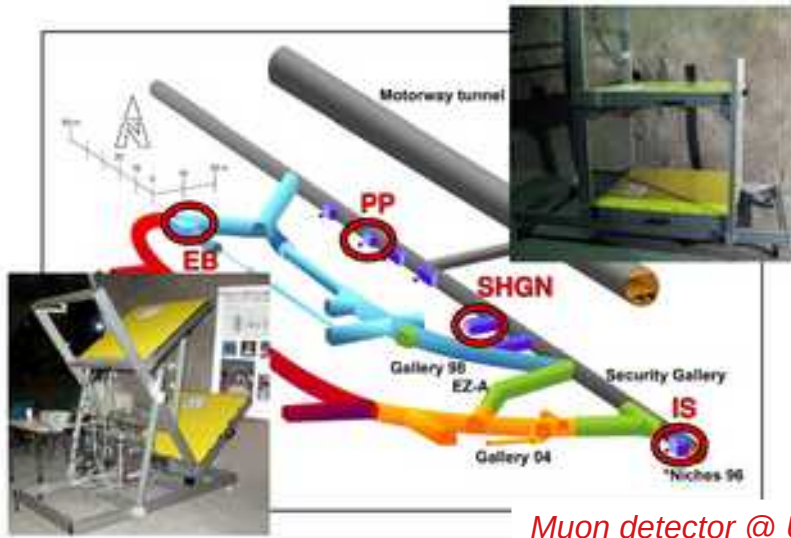
The material is Standard Rock
The step for the curve points is 10 cm

$\text{Height (a)} = 362.9 \pm 0.9 \text{ cm}$

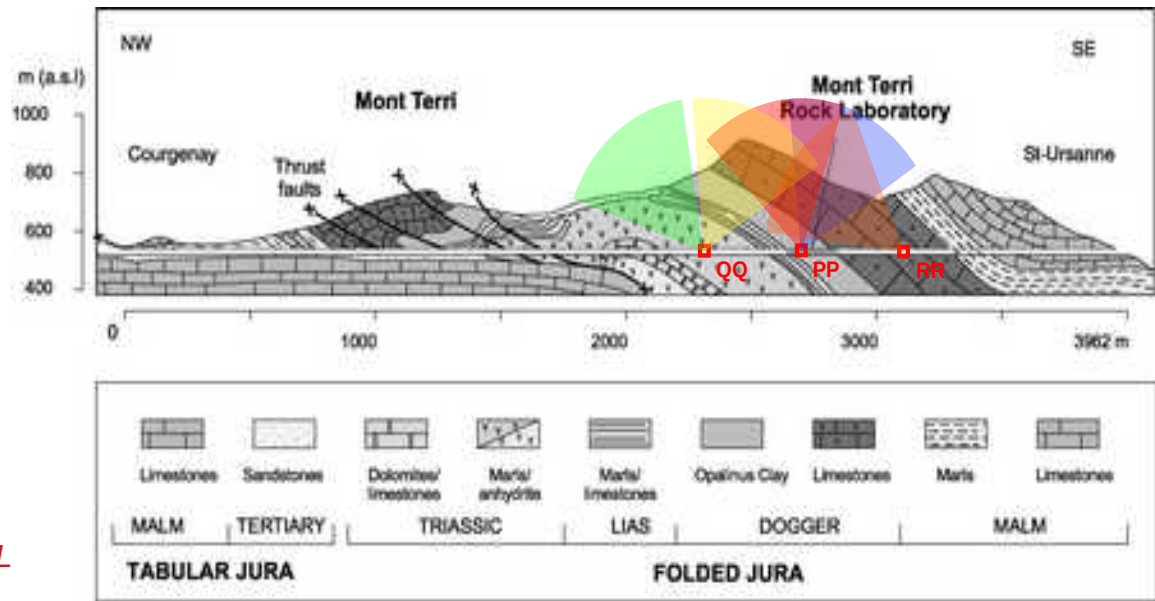
$\text{Height (b)} = 358.4 \pm 0.9 \text{ cm}$

$\langle \text{Height} \rangle = 360.7 \pm 0.6 \text{ cm}$

$\langle \text{Efficiency} \rangle = 0.1524 \pm 0.0004$



Muon detector @ URL



MUON TOMOGRAPHY ACQUISITIONS :

- niche PP - run 1
- niche PP - run 2
- niche QQ - run 3
- niche QQ - run 4
- niche RR - run 5

List of the 2012-2015 runs

Underground labs

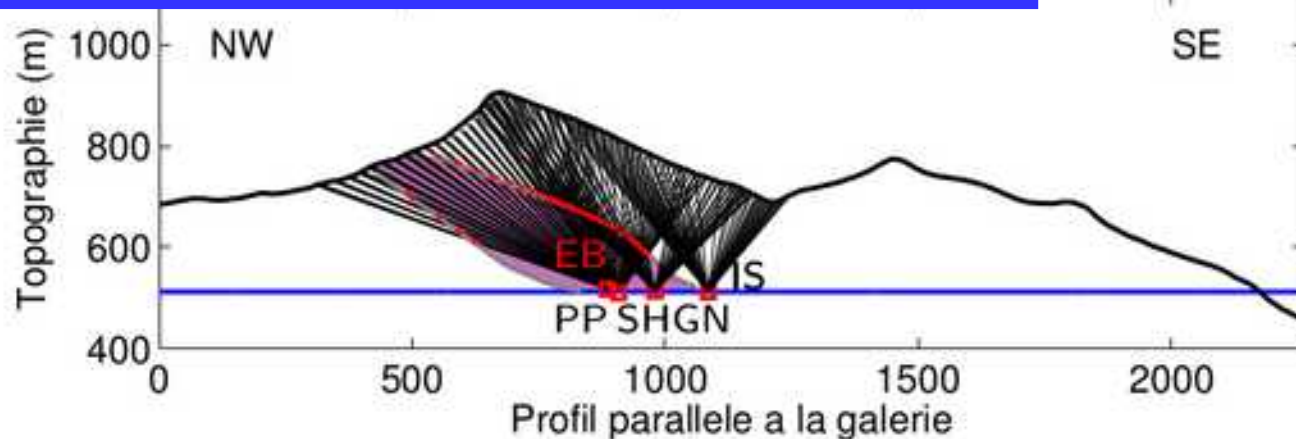


*Muon – gravimetry
joined analysis*



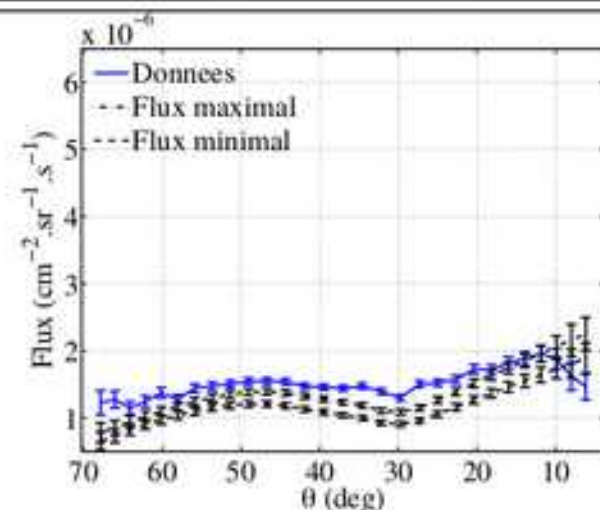
Muon detector @ LSBB

The Mont-Terri lab

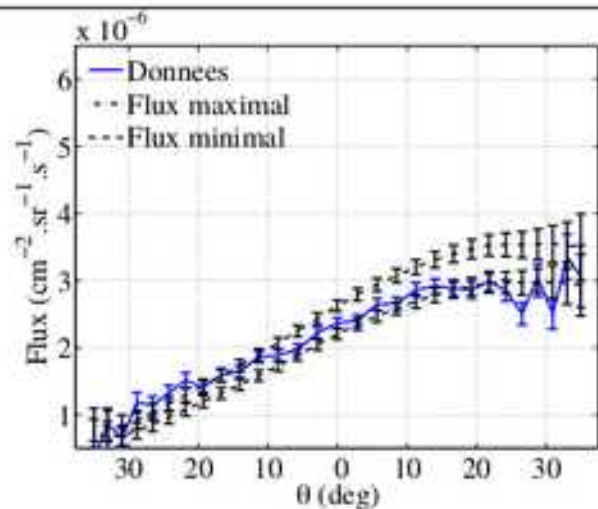


Bruit de fond d'corrél  dans la niche PP : 1.7×10^{-7} /s

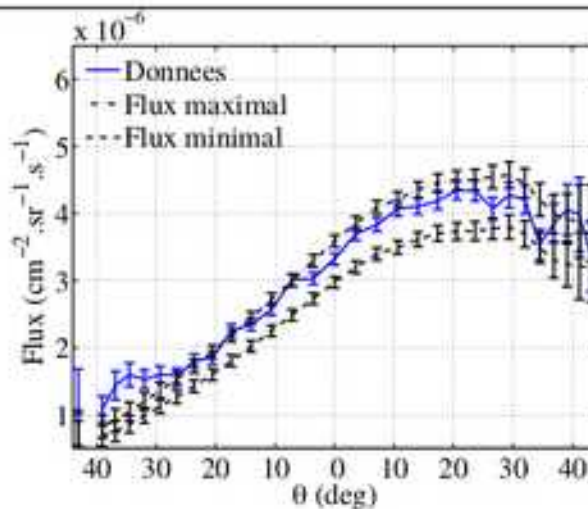
EB (177 jours)



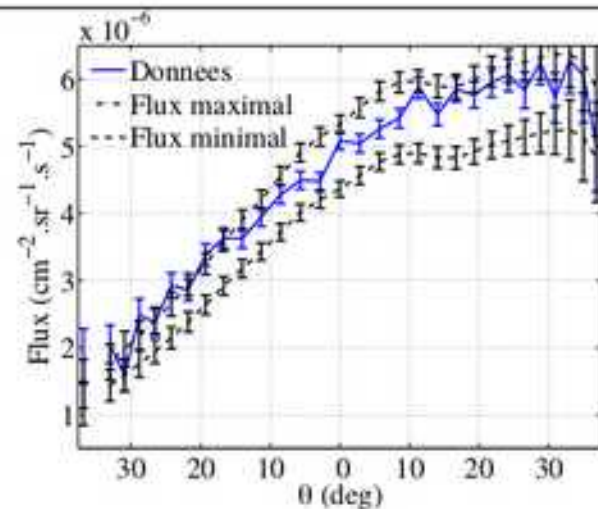
PP (56 jours)



SHGN (42 jours)

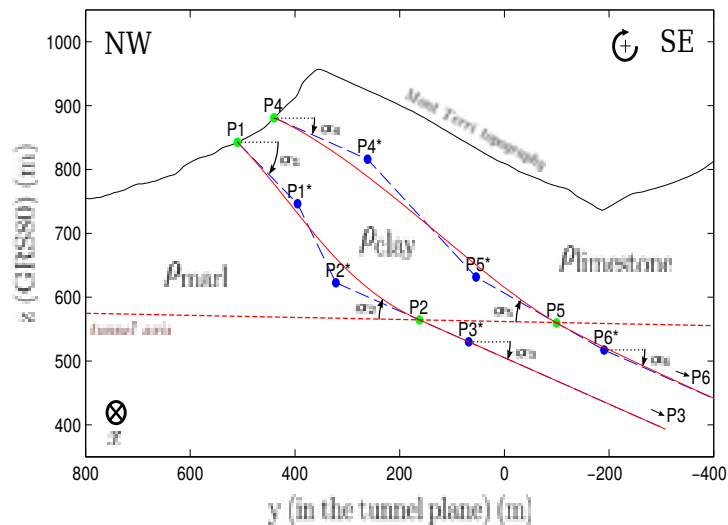


IS (47 jours)

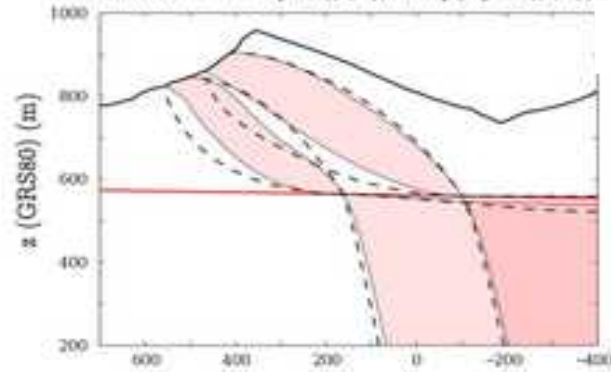


Joint gravi-muon analysis

Opalinus layer parametrization

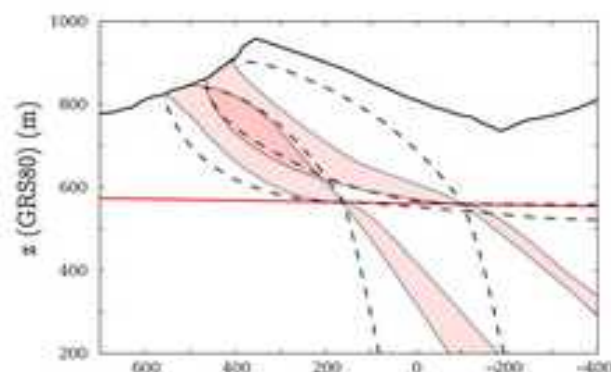
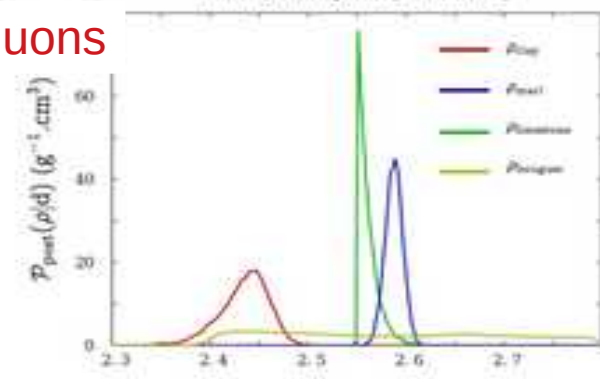


all solutions for $\mathcal{P}_{\rho, \text{ost}}(\rho|d) / \max_{\rho}(\mathcal{P}_{\rho, \text{ost}}(\rho|d)) > 0.6$

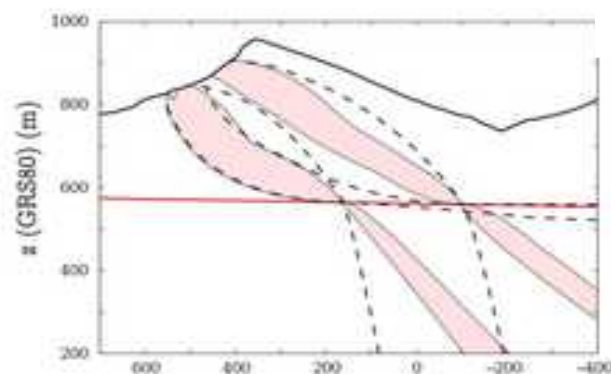
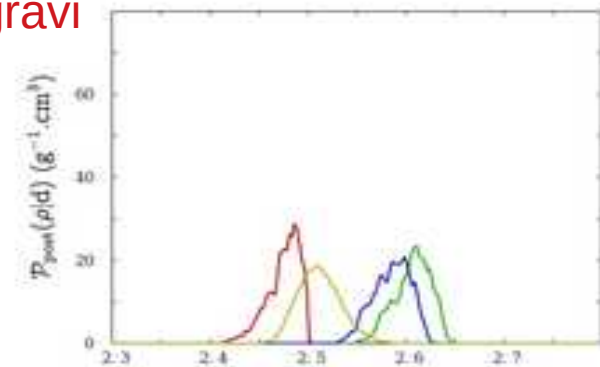


muons

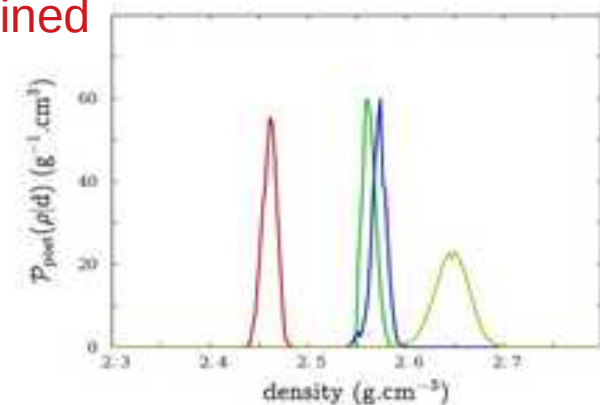
density marginal probability



gravi



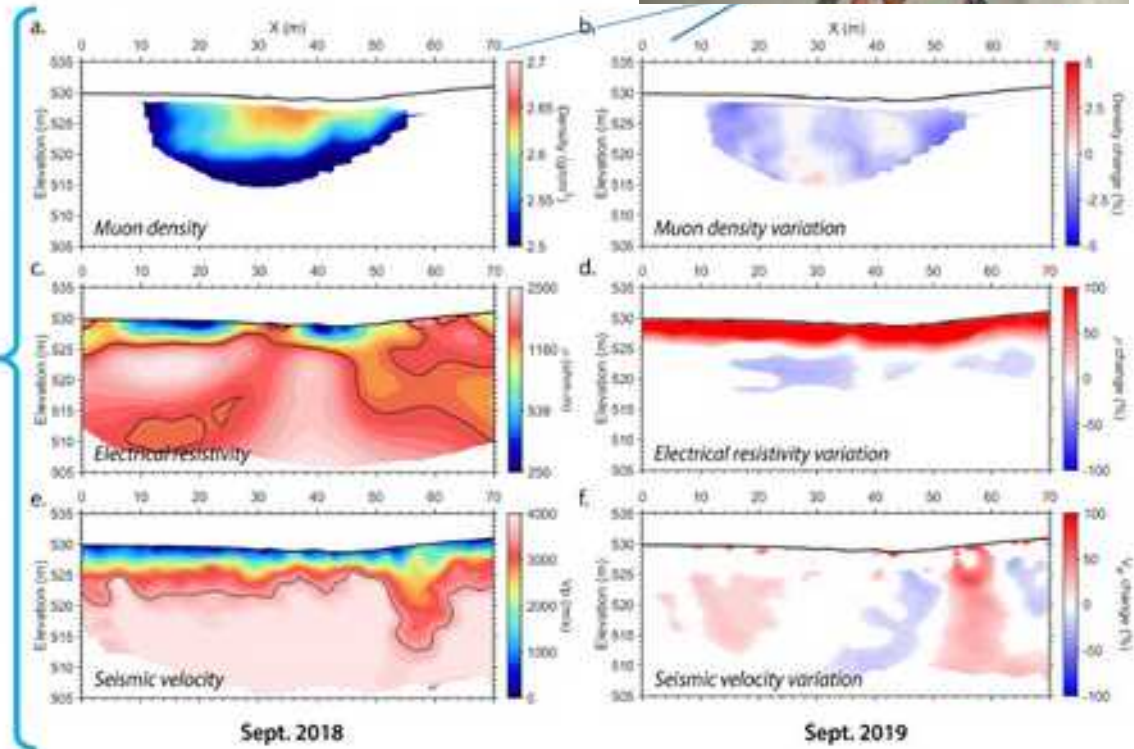
joined



The LSBB facility



A GOOD EXAMPLE: THE BUISSONNIÈRE EXPERIMENT



Ref: Lózaró Roche, I.; Pasquet, S.; Chalikkakis, K.; Mazzilli, N.; Rosas-Carbaljal, M.; Decitre, J.B.; Batiot-Guilhe, C.; Emblanch, C.; Morteau, J. et al. Water resource management: The multi-technique approach of the Low Background Noise Underground Research Laboratory of Rustrel, France, and its moon detection projects. In *Muography: Exploring Earth's Subsurface with Elementary Particles*. 2021, Geophysical Monograph Series; Oláh, L., Tanaka, H., Varga, D., Eds. American Geophysical Union, USA. DOI:10.1002/9781119722748.ch10



The New York Times

INTRODUCED

How Do You See Inside a Volcano? Try a Storm of Cosmic Particles.

Muography, a technique used to peer inside nuclear reactors and Egyptian pyramids, could help map the innards of the world's most hazardous volcanoes.



iP2i
LES 2 INFINIS
LYON

